Spin flux and magnetic solitons in an interacting two-dimensional electron gas: Topology of two-valued wave functions

Sajeev John and Andrey Golubentsev
Department of Physics, University of Toronto, Toronto, Ontario, Canada M5S 1A7
(Received 21 September 1993; revised manuscript received 31 January 1994)

It is suggested that an interacting many-electron system in a two-dimensional lattice may condense into a topological magnetic state distinct from any discussed previously. This condensate exhibits local spin-$\frac{1}{2}$ magnetic moments on the lattice sites but is composed of a Slater determinant of single-electron wave functions which exist in an orthogonal sector of the electronic Hilbert space from the sector describing traditional spin-density-wave or spiral magnetic states. These one-electron spinor wave functions have the distinguishing property that they are antiperiodic along a closed path encircling any elementary plaquette of the lattice. This corresponds to a 2π rotation of the internal coordinate frame of the electron as it encircles the plaquette. The possibility of spinor wave functions with spatial antiperiodicity is a direct consequence of the two-valuedness of the internal electronic wave function defined on the space of Euler angles describing its spin. This internal space is the topologically, doubly-connected, group manifold of SO(3). Formally, these antiperiodic wave functions may be described by passing a flux which couples to spin (rather than charge) through each of the elementary plaquettes of the lattice. When applied to the two-dimensional Hubbard model with one electron per site, this new topological magnetic state exhibits a relativistic spectrum for charged, quasiparticle excitations with a suppressed one-electron density of states at the Fermi level. For a topological antiferromagnet on a square lattice, with the standard Hartree-Fock, spin-density-wave decoupling of the on-site Hubbard interaction, there is an exact mapping of the low-energy one-electron excitation spectrum to a relativistic Dirac continuum field theory. In this field theory, the Dirac mass gap is precisely the Mott-Hubbard charge gap and the continuum field variable is an eight-component Dirac spinor describing the components of physical electron-spin amplitude on each of the four sites of the elementary plaquette in the original Hubbard model. Within this continuum model we derive explicitly the existence of hedgehog Skyrmion textures as local minima of the classical magnetic energy. These magnetic solitons carry a topological winding number μ associated with the vortex rotation of the background magnetic moment field by a phase angle $2\pi\mu$ along a path encircling the soliton. Such solitons also carry a spin flux of $\mu\pi$ through the plaquette on which they are centered. The $\mu = 1$ hedgehog Skyrmion describes a local transition from the topological (antiperiodic) sector of the one-electron Hilbert space to the nontopological sector. We derive from first principles the existence of deep level localized electronic states within the Mott-Hubbard charge gap for the $\mu = 1$ and 2 solitons. The spectrum of localized states is symmetric about $E = 0$ and each subgap electronic level can be occupied by a pair of electrons in which one electron resides primarily on one sublattice and the second electron on the other sublattice. It is suggested that flux-carrying solitons and the subgap electronic structure which they induce are important in understanding the physical behavior of doped Mott insulators.

I. INTRODUCTION

The discovery of high-temperature superconductivity[1] has sparked broad interest in the magnetic properties of strongly correlated electron systems. It was originally suggested by Anderson[2] that a "spin-liquid" phase of strongly interacting electrons may be responsible for many of the anomalous electronic and magnetic features observed in such systems. Experimental evidence[3] for a fundamentally new magnetic phase of this many-electron system comes from the fact that in the absence of any free charge carriers, the oxide superconductors exhibit an antiferromagnetic Mott-Hubbard gap. As charge carriers are introduced by the process of doping, this long range antiferromagnetic order disappears leading to a metallic phase with striking non-Fermi-liquid properties. It is from this parent, metallic phase which superconductivity emerges as the system is cooled. Understanding the nature of this unconventional metal, appears to be the central focus of many-body theory as applied to these systems.[4]

Some insight into the nature of strongly interacting electrons exhibiting magnetic correlations comes from one-dimensional systems.[5,6] Here it is well known that antiferromagnetic spin systems can condense into spin-liquid-type phases consisting of fermionic spin solitons.[7] In the presence of charge carriers these systems may not exhibit Fermi-liquid behavior but rather a Luttinger-liquid behavior.[8] When applying such concepts to the oxide superconductors, which consist of weakly coupled two-dimensional layers, it must be borne in mind that

a continuous change in physical properties takes place in these materials as a function of doping. This change is from manifestly three-dimensional antiferromagnetism at zero carrier concentration, to non-Fermi-liquid or spin-liquid behavior for small carrier concentration and finally to more conventional behavior at high carrier densities.[3] It is possible that spin-liquid behavior in this higher-dimensional system has a fundamentally different microscopic origin than the corresponding spin-liquid states of exactly soluble one-dimensional models.

An attempt to incorporate the three-dimensional antiferromagnetic behavior and Mott-Hubbard band structure into the spin-liquid scenario has been made by Schrieffer *et al.*[9] He suggested that the removal of electrons (addition of holes) to the Mott-Hubbard antiferromagnetic insulator would be accompanied by a local distortion of the antiferromagnetic background. Denoting the local magnetic moment on site i by $\langle \mathbf{s}_i \rangle$, Schrieffer suggested that for weak electron-electron interaction the magnitude of $\langle \mathbf{s}_i \rangle$, and accordingly the magnitude of the Mott-Hubbard gap $\Delta \equiv 2U|\langle \mathbf{s}_i \rangle|$ would be locally suppressed. Here U is the on-site Hubbard repulsion between electrons of opposite spin. This leads to a magnetic polaronlike state (spin bag) for the charge carrier. On the other hand, Shraiman and Siggia[10] noted that in the large-U limit the charge carrier may lower its energy more easily by a local distortion of the orientation of $\langle \mathbf{s}_i \rangle$ while keeping the magnitude $s \equiv |\langle \mathbf{s}_i \rangle|$ fixed. They suggested that a single charge carrier would be accompanied by a dipolar texture in the magnetic background. A global twist of the magnetic background also leads to a change of the overall Mott-Hubbard effective one-electron band structure. Mean-field theories have verified that for a uniform density, δ, of charge carriers (holes), a small deviation $\mathbf{q}$ of the wave vector describing magnetic order from that of the antiferromagnetic order leads to a lowering of the kinetic energy of charge carriers by an amount of order $-t\delta(qa)$. Here t is the intersite hopping matrix element for electrons and a is the lattice constant. The pitch, q, of the resulting spiral magnetic state leads to an increase in the classical magnetic exchange energy. If we denote the antiferromagnetic exchange energy scale t^2/U by J, then this increase in magnetic energy scales as $+J(qa)^2$. It follows that a twisted magnetic state whose spiral pitch q increases continuously with δ minimizes the total energy.

Both of the above pictures utilize the fact that the Mott-Hubbard system is analogous to a doped semiconductor in which the electronic band structure is sensitively determined by the magnetic moment background. In the spin-bag scenario sensitivity to the magnitude, s, was considered whereas in the spiral magnetic phases, this sensitivity was extended to the order parameter space S_2 (surface of a unit sphere) describing the local magnetic moment orientation. In this paper we point out that the Mott-Hubbard band structure may in fact be sensitive to a larger order parameter space than the sphere S_2. This is because the Mott-Hubbard semiconducting gap is sustained, not by a collection of classical magnetic moments, but rather by a background field of spin-$\frac{1}{2}$ electrons. The underlying classical order parameter space which gives rise to spin $\frac{1}{2}$ is not the sphere S_2 but rather the entire group manifold of SO(3) describing the group of rotations in three dimensions. Physically, what distinguishes these two manifolds is the fact that there is a meaningful phase factor to the electronic wave functions comprising the magnetic background and that this phase can severely affect the band structure independently of the actual local moment orientation. This phase corresponds to a rotation of the underlying electron spinor field about the axis $\langle \hat{s}_i \rangle$ of the local moment itself. It can be regarded as the third Euler angle associated with the electron's internal coordinate frame in addition to the two Euler angles which define the axis $\langle \hat{s}_i \rangle$. We show that these considerations give rise to a topological variant of the conventional spin-density-wave and spiral magnetic states of the Hubbard model. The effects of this additional phase degree of freedom can be incorporated by introducing the notion of "spin flux." This "spin flux" corresponds to a homotopically nontrivial phase rotation of the electron spinor around a closed trajectory in coordinate space. This, for instance, could occur if the internal coordinate system of the electron undergoes a 2π rotation as the electron encircles an elementary plaquette of the two-dimensional square lattice. For simplicity, we consider a uniform topological magnetic condensate in which the local moment structure is that of an antiferromagnet and an elementary unit of spin flux penetrates each plaquette of the lattice. We will show later that spin flux can be dynamically generated by the nucleation of a vortex-antivortex pair in the local magnetic moment background. In this case a drastic modification of the effective one-electron band structure takes place in which the conventional nested Fermi surface for the two-dimensional square lattice collapses to a set of four Fermi points which occur at the corners of the square Brillouin zone of the spin flux phase. A continuum theory for charged, quasiparticle excitations near these Fermi points maps exactly to a (2+1)-dimensional relativistic Dirac field theory. Here, the "Dirac mass gap" is precisely the Mott-Hubbard gap $\Delta = 2Us$ and the "Dirac spinor" is an eight-component field variable which describes the two components of electron-spin amplitude on each of the four lattice sites of an elementary plaquette. This mapping is an illustration of the mathematical connection between topology, relativity and the spin-statistics theorem. Within this spin flux phase, we demonstrate the natural occurrence of hedgehog, Skyrmion textures in the local moment background as well as the subgap electronic structure which they induce. These textures induce phase vorticity in the magnetic background and may be regarded as topological solitons. A proliferation of such solitons in the presence of charge carriers is suggested as an alternative to conventional spiral antiferromagnetism and as a possible scenario for spin-liquid behavior.

In Sec. II, we present a brief review of the topology and underlying two-valuedness of spin-$\frac{1}{2}$ wave functions. In Sec. III, we derive from first principles the electronic structure of the uniform spin-flux phase and its mapping to a (2+1)-dimensional continuum field theory. Finally in Sec. IV, we show that subgap electronic structure may

be induced by the presence of topological magnetic solitons and we present a numerical study of the resulting electronic spectrum.

II. WAVE FUNCTIONS FOR SPIN-$\frac{1}{2}$ ELECTRONS

In this section, we describe an extension and generalization of the physical Hilbert space of an interacting many-electron system. This extension is consistent with the fundamental axioms of quantum mechanics as applied to spin-$\frac{1}{2}$ particles, but to our knowledge has not been discussed previously in the context of many-body theory in condensed matter physics. This extension is relevant and perhaps essential to the understanding of strongly correlated electron systems in which local magnetic moments appear, and with which the charge degrees of freedom of the electron gas must interact. All of the consequences of this extension which we describe, such as the spontaneous appearance of SU(2) spin flux in the many-electron system, the relativistic dispersion relation of charged quasiparticles in two dimensions, and the natural occurrence of flux-carrying magnetic solitons are precise and direct consequences of the axioms of quantum theory and the topology of the physical rotation group SO(3).

Elementary particles in physical three-dimensional space are divided into two fundamental classes: bosons and fermions. The origin of this dichotomy may be regarded purely as a geometrical property of physical three-dimensional space. This is evident from a direct application of the axioms of quantum mechanics to the space of Euler angles describing the local or internal coordinate frame of the particle.[11,12] This set of Euler angles is a parametrization of the manifold of the compact Lie group SO(3). If we label the three Euler angles as (η_1, η_2, η_3), then geometry alone specifies the metric tensor g_{ij} on this group manifold by the relations $g_{11} = g_{22} = g_{33} = 1$ and $g_{23} = g_{32} = \cos\eta_1$. All other components are zero. This fact is sufficient to specify classical mechanics within this manifold. For instance the rotational kinetic energy of a symmetrical spinning top (whose rotational kinematics is completely specified within the space of Euler angles) is given by[13]

$$L_{\text{internal}} = \frac{I}{2}\sum_{ij} g_{ij}\dot{\eta}_i\dot{\eta}_j \ . \tag{2.1}$$

Here $\dot{\eta}_i \equiv \frac{\partial}{\partial t}\eta_i$, I is the moment of inertia, and t is the time variable. This specification is simply an expression of the fact that classical motion follows the geodesic paths[12] within the group manifold SO(3). The rules of canonical quantization then determine the precise form of all internal wave functions describing the various states of intrinsic spin angular momentum which this object can possess. Defining the classical conjugate momenta, $p_i \equiv \partial L/\partial\dot{\eta}_i$, and imposing the quantization condition $[\eta_\alpha, p_\beta] = i\hbar\delta_{\alpha\beta}$ leads to a Schrödinger equation (see Appendix A)

$$H_{\text{internal}}\Psi_{\text{internal}} = E\Psi_{\text{internal}} \ . \tag{2.2}$$

Here H_{internal} is simply the Laplacian operator on SO(3) and the wave function $\Psi_{\text{internal}}(\boldsymbol{\eta})$ may be interpreted as a transformation amplitude[14] for a component of spin when the quantization axes are rotated by the set of internal Euler angles $\boldsymbol{\eta}$. The axioms of quantum mechanics require that Ψ_{internal} must be a continuous, differentiable function and that $|\Psi_{\text{internal}}|^2$ must be single-valued. It follows immediately that this wave function can describe only integer or half-integer spins. For example, a solution of the internal Schrödinger equation describing a spin angular momentum of $\hbar/2$ is given by $\Psi_{\text{internal}}(\boldsymbol{\eta}) = \cos(\eta_1/2)\exp[i(\eta_2 + \eta_3)/2]$. This wave function is a two-valued, continuous function. Clearly, under a continuous 2π rotation ($\eta_i \to \eta_i + 2\pi$) the wave function changes sign and so both Ψ_{internal} and $-\Psi_{\text{internal}}$ must be associated with any given point $\boldsymbol{\eta}$ of the group manifold SO(3). The fact that motion along a continuous closed path in the group manifold can continuously change the value of the wave function by a factor of $e^{i\pi}$ without the presence of a singularity is a consequence of the doubly connected topology of SO(3). The group manifold may be depicted as a solid ball of radius π with the antipodal points identified (see Fig. 1). With each point on the sphere, we associate a rotation matrix. The axis on which the point lies defines the axis of rotation and the distance of the point from the origin defines the angle of rotation. There are two homotopically nonequivalent classes of closed paths that may be traversed within this manifold: those which cross the surface of the sphere and those which do not. The fact that the former cannot be continuously deformed to zero is what allows the wave function to be both two-valued as well as everywhere continuous and differentiable.

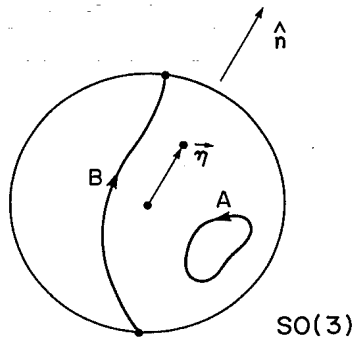

FIG. 1. The group manifold of SO(3) is depicted as a solid ball of radius π. There is a 1:1 correspondance between points $\boldsymbol{\eta} = \rho\hat{n}$ in this manifold and physical rotation matrices $T \equiv \exp(i\boldsymbol{\eta}\cdot\boldsymbol{\sigma}/2)$ which describe a rotation about the axis $\hat{n}$ by an angle ρ. Since a rotation by π is equivalent to a rotation by $-\pi$, the antipodal points of the solid ball must be identified. Two homotopically, nonequivalent paths A and B within this manifold are depicted. Path A can be continuously deformed to a single point whereas path B cannot. Spin flux arises when the internal coordinate frame of an electron traverses the path B during the course of a closed trajectory in external coordinate space.

From the previous argument, it is apparent that the internal electron wave function exhibits antiperiodicity along any internal path [within SO(3)] which crosses the surface of the group manifold (Fig. 1) once. The question whether this antiperiodicity can manifest itself for a closed path in external coordinate space, however, has not been addressed in the context of many-body theory. For this to occur, the electron would need to undergo spin-dependent scattering along its coordinate space trajectory, in such a way that its internal coordinate space was rotated by 2π (see Fig. 2). For the conventional spin-density-wave state, spin-dependent scattering occurs by virtue of a coherent or condensed state of the electron gas in which the electron spin operator acquires a nonzero expectation value. Scattering from this local magnetic moment background, gives a nontrivial spatial dependence to the effective one-electron wave functions which make up the many-body state. A simple example is a two-dimensional spiral magnetic state of wave vector $\mathbf{Q}$ polarized in the x-y plane.[15] Defining $(1,0)$ as the spinor for a $+\hbar/2$ state in the $\hat{z}$ direction, such a state is composed of one-electron wave functions of the form $\chi_{\mathbf{k}}(\mathbf{r}) = [\cos\theta(\mathbf{k})e^{i\mathbf{k}\cdot\mathbf{r}}, \sin\theta(\mathbf{k})e^{i(\mathbf{k}+\mathbf{Q})\cdot\mathbf{r}}]$. Here, $\mathbf{r}$ is the position of the electron in the two-dimensional Euclidean space, $\sin\theta$ and $\cos\theta$ are spin amplitudes for an electron of wave vector $\mathbf{k}$ and the many-body wave function consists of a Slater determinant of such states taken over a Fermi sea of wave vectors. This can be rewritten as

$$\chi_{\mathbf{k}}(\mathbf{r}) = e^{i(\mathbf{k}+\mathbf{Q}/2)\cdot\mathbf{r}} e^{-i\eta_3(\mathbf{r})\sigma_z/2} \begin{pmatrix} \cos\theta(\mathbf{k}) \\ \sin\theta(\mathbf{k}) \end{pmatrix} , \quad (2.3)$$

where $\eta_3(\mathbf{r}) = \mathbf{Q}\cdot\mathbf{r}$. In this simple model, it is clear that as the electron traverses any continuous closed path in the external coordinate space $\mathbf{r}$, its internal coordinate frame undergoes a continuous rotation by the Euler angle $\eta_3(\mathbf{r})$ which is topologically trivial: the function $\eta_3(\mathbf{r})$ is path independent and single-valued.

In the two-dimensional square lattice, the spiral, spin-density-wave state is periodic with respect to 2π rotations in coordinate space and the many-electron wave function lies in what we call the nontopological sector of the Hilbert space. Let R_z^{ext} be an operator which rotates the electron's external coordinate $\mathbf{r}$ by an angle of 2π about an axis $\hat{z}$ which pierces the center of some particular plaquette of the square lattice. Then $R_z^{\text{ext}}|\chi_{\mathbf{k}}\rangle = |\chi_{\mathbf{k}}\rangle$. For $\mathbf{Q} = \mathbf{Q}_0 \equiv \frac{\pi}{a}(1,1)$ (where a is the two-dimensional lattice constant), and a suitable choice of $\theta(\mathbf{k})$, the corresponding Slater determinant wave function describes a Néel antiferromagnet polarized in the $\pm\hat{x}$ direction. A topological variant of this state, $|\chi_{\mathbf{k}}^{\text{topol}}\rangle$ with precisely the same local magnetic moment structure is obtained by applying a spatially varying phase rotation to the underlying one-electron spinor states:

$$\chi_{\mathbf{k}}^{\text{topol}}(\mathbf{r}) \equiv e^{-i\eta_1(\mathbf{r})\sigma_x/2}\chi_{\mathbf{k}}(\mathbf{r}), \quad (2.4a)$$

where the Euler angle field is given by

$$\eta_1(\mathbf{r}) = \int_{\mathbf{r}_0}^{\mathbf{r}} \mathbf{A}\cdot d\boldsymbol{\ell} \ , \quad (2.4b)$$

$$\mathbf{A}(\mathbf{r}) = \sum_j (-1)^j \mathbf{A}_1(\mathbf{r}-\mathbf{R}_j) \ , \quad (2.4c)$$

and

$$\mathbf{A}_1(\mathbf{r}) = \frac{\hat{\theta}}{r} \ . \quad (2.4d)$$

Here, the line integral (2.4b) runs from some arbitrary reference point $\mathbf{r}_0$ to the point in question $\mathbf{r}$. The "vector potential," $\mathbf{A}(\mathbf{r})$, is the sum of vector potentials $\mathbf{A}_1(\mathbf{r})$ arising from solenoids placed at the center, $\mathbf{R}_j$, of each plaquette (see Fig. 3). $\hat{\theta}$ is a unit tangential vector perpendicular to the coordinate vector $\mathbf{r}$. This corresponds to a vortexlike phase rotation of the electron spinor field about the local axis of magnetization $\hat{x}$ around each solenoid. While preserving the antiferromagnetic ordering, this transformation describes a phase change of $e^{i\pi}$ along any closed path in $\mathbf{r}$ space which encircles an odd number of elementary plaquettes. The

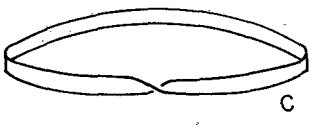

FIG. 2. An antiperiodic spin-$\frac{1}{2}$ wave function may be pictured as a Mobius strip. The two sides of the strip correspond to the two values of the spinor wave function $\pm\chi$. A closed electron trajectory, C, in coordinate space corresponds to a trajectory around the strip. As the electron encircles the closed loop, C, the value of its wave function switches continuously from $+\chi$ to $-\chi$.

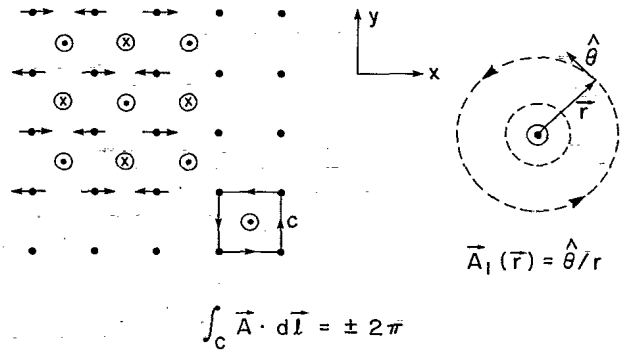

FIG. 3. A topological variant of an $\hat{x}$-polarized antiferromagnetic spin-density-wave state is shown. Here the one-electron spinor wave functions have been given a topologically nontrivial phase rotation about $\hat{x}$ by an Euler angle field $\eta_1(\mathbf{r})$. This field is path dependent and may be regarded as the line integral of a fictitious vector potential. The vector potential arises from placing a solenoid at the center of each plaquette. The resulting wave function is antiperiodic along a closed path, C, that encircles any elementary plaquette. This is analogous to the π twist in a Mobius strip.

inherent two-valuedness of the internal electronic wave functions (in the space of Euler angles) is now manifest as a two-valuedness in external coordinate space. This two-valuedness is defined by the fact that $R_z^{\rm ext}|\chi_{\mathbf{k}}^{\rm topol}\rangle = -|\chi_{\mathbf{k}}^{\rm topol}\rangle$, and we refer to these one-electron spinor wave functions as being completely antiperiodic. Moreover, in the absence of electromagnetic coupling, there is no elementary one-electron matrix element which connects a periodic wave function to an antiperiodic one. Let A be any one-electron operator which is invariant under a 2π rotation. Since $R_z^{\rm ext} = (R_z^{\rm ext})^{-1}$ and $R_z^{\rm ext} A R_z^{\rm ext} = A$, it follows that $\langle\chi_{\mathbf{k}}^{\rm topol}|A|\chi_{\mathbf{k}}\rangle = \langle\chi_k^{\rm topol} R_z^{\rm ext}|A|R_z^{\rm ext}\chi_k\rangle = -\langle\chi_{\mathbf{k}}^{\rm topol}|A|\chi_{\mathbf{k}}\rangle$. Therefore, $\langle\chi_{\mathbf{k}}^{\rm topol}|A|\chi_{\mathbf{k}}\rangle = 0$, and a quantum-mechanical transition of a single electron from the nontopological sector of the Hilbert space to the topological one is strictly forbidden. As we will show in Sec. IV, a one-electron transition from a state which is periodic to one which is antiperiodic about a given plaquette (or vice versa) requires the motion of an elementary unit of spin vorticity of the local moment background to or from this plaquette. This spin vorticity is in fact carried by magnetic solitons (Skyrmions) which are free to move in the two-dimensional lattice. The soliton creation operator, $V^\dagger$, involves a rotation of the internal spinor states of electrons from 0 to 2π around a closed loop in coordinate space which encircles the soliton core. It follows that under a 2π rotation in external coordinate space, this creation operator in fact satisfies the property $R_z^{\rm ext} V^\dagger R_z^{\rm ext} = -V^\dagger$. Soliton motion requires rearrangement of the phases of all of the other electrons in the many-body system and is mediated by the Coulomb interaction. Accordingly, we expect that strong electron-electron interaction is an essential prerequisite for the occurrence of the topological effects which we describe in this paper. The soliton states as well as spin-flux background may be regarded as a new variational wave function which describes spin-dependent scattering and the resulting many-body correlations.

III. SPIN-FLUX STATE OF THE 2D HUBBARD MODEL

In a recent series of papers,[16–18] we have presented a careful study of the magnetic and electronic properties of the strongly correlated Hubbard model starting from a mean-field theory of spiral magnetism and continuing to the lowest-order fluctuation corrections. This was based on the viewpoint that in a physical system such as the layered high-T_c oxide superconductors, the exact behavior of the two-dimensional Hubbard model was modified by weak interlayer couplings. Based on the experimental observation of long range antiferromagnetic order in these materials, we assumed that the effect of weak interlayer couplings was to stabilize mean-field approximations to the two-dimensional model: although the Mermin-Wagner theorem[19] forbids long range order at finite temperature in two dimensions, these mean-field approximations provided a useful starting point for describing the actual physical system at small values of the carrier concentration δ ($1-\delta \equiv$ average electron occupation per site). As the carrier concentration δ is increased from zero, magnetic order disappears within these layered materials. In our approach, this disappearance of long range order is associated with fluctuation corrections to mean-field theory which tend to restore broken symmetry. Evidence for underlying magnetic correlations which have been disrupted by fluctuations comes from magnetic neutron scattering.[20–23] Inelastic neutron scattering peaks are observed in $Y_1Ba_2Cu_3O_{7-\delta}$ at the antiferromagnetic wavevector $\mathbf{Q}_0 \equiv \frac{\pi}{a}(1,1)$. Here, a is the lattice constant for the square lattice. For the related compound, $La_{2-\delta}Sr_\delta CuO_4$, antiferromagnetism is observed at $\delta = 0$, but inelastic neutron scattering peaks appear for nonzero doping at $\mathbf{Q} = \mathbf{Q}_0 + \mathbf{q}$ where the deviation vector takes on four possible values $\mathbf{q} = \pm q(1,0)$ and $\pm q(0,1)$. The magnitude of the spiral pitch q varies continuously with doping δ. Experimental data on this variation of pitch with doping[23] can be fitted to the corresponding spiral magnetic mean-field theory of the Hubbard model.[17,18] The fit is accurate for a ratio of on-site electron-electron interaction U to hopping matrix element t which is in the range of 4–6. This is not inconsistent with the occurrence of domains of short range ordered spiral magnetism in which the size of the domains is slightly larger than the average spacing between charge carriers. This could arise from actual domain walls separating various degenerate spiral states or from some other nonlinear fluctuation effect.

Another independent experimental signature which is consistent with mean-field theory is the dependence of the Hall coefficient R_H with doping δ.[1,24] In $La_{2-\delta}Sr_\delta CuO_4$, it is observed that R_H changes sign for $\delta \simeq 0.18$. Remarkably, this behavior can also be described using nearly the same Hubbard model parameters as before.[18] The sign change, in this picture, is a natural consequence of the evolution of the Fermi surface topology with doping. For small doping, there is a small Fermi surface with a positive (holelike) R_H whereas for larger δ, this evolves into a large Fermi surface with an (electronlike) negative R_H. The precise value of δ at which R_H passes through zero is determined by the ratio U/t and the nature of the spiral magnetic mean-field background. In effect, the changes in spiral magnetic pitch and the magnitude of local moment formation with doping δ, induce significant modifications of the effective one-electron band structure. With the choice of $U/t \sim 4-6$, the Mott-Hubbard semiconducting gap which appears at $\delta = 0$ evolves into an indirect gap for $\delta > 0$ and eventually disappears entirely at around $\delta = 0.3$ within this mean-field picture. This eventual closure of the Mott-Hubbard gap for large doping is also consistent with the reappearance of metallic (Fermi-liquid) behavior for doping $\delta > 0.3$, in the copper-oxide materials.

Although mean-field theory describes certain general electronic and magnetic features of these materials, it is fundamentally inadequate in describing key features of the parent phase, from which superconductivity emerges (as the temperature is lowered). These key features are entailed in the marginal-Fermi-liquid hypothesis and phenomenology.[25,26] Among the nearly universal anoma-

lies contained in this phenomenology are the unusual temperature dependence of the Hall coefficient, the persistence of linear temperature behavior in the ordinary resistivity, and the striking broadband midinfrared absorption within the Mott-Hubbard gap. Neither mean-field theory nor its lowest-order fluctuation (spin-wave or spin-charge collective mode) corrections[17] can account for these effects.

The glaring persistence of non-Fermi-liquid anomalies as well as the inadequacy of conventional mean-field theories of the Hubbard model to address them has led us to ask whether the underlying two-valued nature of spin-$\frac{1}{2}$ wave functions may lead to anomalies at a very fundamental level which have hitherto been unexplored.[27] We begin by describing the spin-flux or topological antiferromagnetic state. This state is a variant of the conventional spin-density-wave mean-field state in which the underlying one-electron spinor wave functions are forced to be antiperiodic around *each* of the elementary plaquettes of the square lattice. This uniform spin-flux state may be regarded as an alternative mean-field ground state of the Hubbard model. As we describe in Sec. IV, the existence of such a state introduces the possibility of topological fluctuation corrections to the conventional antiferromagnet. In fact we show that magnetic hedgehog (Skyrmion) solitons locally interpolate between these two ground states. That is to say, a topological soliton centered on a given plaquette of the two-dimensional (2D) lattice changes the symmetry of one-electron states encircling this plaquette from periodic to antiperiodic or vice versa. The structure of the hedgehog is such that this local tunneling event also inverts the local magnetic moment structure near its center. As such, these solitons may lead to a rapid destruction of long range antiferromagnetic order. In this paper, we point out the kinematic possibility of such effects from a microscopic point of view, but leave the detailed energetics and resulting dynamical consequences to a future publication. One remarkable feature is the conversion of the conventional, anisotropic, Mott-Hubbard, band structure in 2D into a quasirelativistic one.

From the standpoint of second quantization, the topological structure of the many-electron Hilbert space may be described by considering the set of all physically admissible local gauge transformations on the Hubbard model:[28,29]

$$\mathcal{H} = -t \sum_{\substack{\langle ij \rangle \\ \alpha}} \left[b^{\dagger}_{i\alpha} b_{j\alpha} + h \cdot c \cdot \right] + U \sum_{i} n_{i\uparrow} n_{i\downarrow} . \tag{3.1}$$

Here $b^{\dagger}_{i\alpha}$ creates an electron at site i of spin α. We consider a local gauge transformation on this operator which implements an Euler angle rotation of the electron's internal coordinate system. Denoting the three Euler angles by $\boldsymbol{\eta}_i = (\eta_{1i}, \eta_{2i}, \eta_{3i})$, we define the rotated electron operator $c^{\dagger}_{i\alpha}$ by the relation $b^{\dagger}_{i\alpha} \equiv [e^{i(\boldsymbol{\eta}_i \cdot \boldsymbol{\sigma})/2}]_{\alpha\beta} c^{\dagger}_{i\beta}$. Here $\boldsymbol{\sigma} \equiv (\sigma^1, \sigma^2, \sigma^3)$ are the three Pauli spin matrices and there is an implicit summation over the repeated index β. It is clear that such a substitution leaves the interaction term invariant. However, if the Euler angle field $\boldsymbol{\eta}_i$ varies with index i, the electron hopping terms will be modified. Defining a SU(2) gauge field $\mathbf{A}^{\mu}$ by the relation

$$(\eta_{\mu i} - \eta_{\mu j}) \sigma^{\mu}_{\alpha\beta} = \int_i^j d\boldsymbol{\ell} \cdot \mathbf{A}^{\mu} \sigma^{\mu}_{\alpha\beta} \tag{3.2}$$

the gauge-transformed Hamiltonian becomes

$$\mathcal{H} = \sum_{\langle ij \rangle} [c^{\dagger}_{i\alpha} T^{ij}_{\alpha\beta} c_{j\beta} + \text{H.c.}] + U \sum_i n_{i\uparrow} n_{i\downarrow} , \tag{3.3a}$$

where the hopping coefficient t for the link $\langle i, j \rangle$ has been replaced by the SU(2) matrix

$$T^{ij} = \exp\left(i/2 \int_i^j d\boldsymbol{\ell} \cdot \mathbf{A}^{\mu} \sigma^{\mu} \right) . \tag{3.3b}$$

Here, we assume for simplicity that each of the Euler angle rotations is about some fixed axis $\hat{n}$.

There is a crucial difference between the nature of physically admissible gauge transformations for spin-$\frac{1}{2}$ electrons and those familiar from elementary scalar quantum mechanics. In the latter case, the wave function $\psi(\mathbf{r})$ is required to be single-valued in three-dimensional Euclidean space. A relabeling of the phase of the wave function $\psi \rightarrow \exp[i\theta(\mathbf{r})\psi]$, leads to the introduction of a U(1) gauge field into the Schrödinger equation. Provided that the gauge field is chosen to have the form $\mathbf{A} = \boldsymbol{\nabla}\theta$ for some single-valued field $\theta(\mathbf{r})$, the spectrum is unchanged. The introduction of more general configurations of the gauge field for which $\boldsymbol{\nabla} \times \mathbf{A} \neq 0$, however, corresponds to the addition of electromagnetic forces. As described in Sec. II, for the case of spin-$\frac{1}{2}$ electrons, the internal wave function defined on the space of Euler angles is *two-valued*. There are two distinct spinors which describe the same physical rotation of the electron and two distinct SU(2) matrices, $\pm T$, which describe the same physical rotation of the electron's internal coordinate system. This is a direct consequence of the doubly connected topological nature of the group manifold of SO(3). It follows that the one-electron spinor wave function $\chi^{\dagger}(\mathbf{r}) \equiv [\phi^*_{\uparrow}(\mathbf{r}), \phi^*_{\downarrow}(\mathbf{r})]$ describing the up- and down-spin amplitudes can be relabeled at each point in space by a local SU(2) gauge transformation $\chi \rightarrow T(\mathbf{r})\chi$ which creates a phase change of either ± 1 for any closed loop in the coordinate space $\mathbf{r}$. In other words, the product of SU(2) matrices in (3.3a) $T^{12}T^{23}T^{34}T^{41}$, describing hopping around an elementary plaquette can be chosen to be either ± 1. In the case of a phase change $e^{i\pi}$, it is apparent that $\boldsymbol{\nabla} \times \mathbf{A} \neq 0$. Nevertheless, we postulate that such a gauge field is admissible without the introduction of an external Yang-Mills force. It does, however, describe a distinct topological sector of the many-electron Hilbert space which may be accessible in the presence of strong electron-electron interactions.

The choice $T^{12}T^{23}T^{34}T^{41} = -1$ describes a singular gauge transformation and consequently is *not* a unitary transformation of the Hamiltonian on the conventional Hilbert space of periodic wave functions. The appearance of the spin flux in the Hubbard Hamiltonian may be regarded as the introduction of a variational many-

body wave function that spans not only the conventional Hilbert space but the extended Hilbert space which includes both periodic and antiperiodic wave functions. The SU(2) gauge field which enters the kinetic energy is simply a mathematical bookkeeping device for keeping track of symmetry changes in the wave function around specific plaquettes. Similar mathematical devices have been employed in U(1) charge-flux phases of the t-J model,[30,31] the resonating-valence-bond model[32] and the anyon model.[33] In the charge-flux variational wave functions, the U(1) gauge field affects both up- and down-spin electrons identically. It is equivalent to the vector potential describing physical electromagnetism. Although the electromagnetic interaction is not explicitly present in the Hubbard model, its effect enters through the variational wave function on which Hubbard Hamiltonian acts. Transitions from a zero-flux state to a U(1) charge-flux state may be regarded as a consequence of vacuum fluctuations of the physical electromagnetic field.[34]

In the case of spin flux, the SU(2) gauge field [Eq. 3.3b] is coupled to the Pauli spin matrices. As a result, there are no static charge currents or magnetic fields associated with our variational wave function. The dynamical generation of spin flux may nevertheless arise from transient fluctuations in the many-body system coupled to physical electromagnetism. For example, a current fluctuation in the many-electron system with a toroidal symmetry can spontaneously create a conventional charge-flux of π and $-\pi$, respectively, on two adjacent plaquettes. In the presence of such a quantum fluctuation, both up- and down-spin electrons encircling the first plaquette will acquire a phase of $e^{i\pi}$. Since this is equivalent to a phase of $e^{-i\pi}$, such a charge-flux fluctuation can trigger a nonzero transition matrix element between the nonflux state and the spin-flux state. The change in flux by 2π in one spin component is equivalent to a radiative transition accompanied by a spin flip. After this tunneling process takes place, the currents and magnetic fields may subside, leaving behind a spin flux of π and $-\pi$ on the adjacent plaquettes. The nonunitary modification of the kinetic energy simply keeps track of those plaquettes in which our trial wave function has undergone a change in symmetry from periodic to antiperiodic.

An alternative, but weaker, mechanism for dynamical spin-flux generation comes from a many-body generalization of the spin-orbit coupling. As in the case of electromagnetism, this interaction does not appear explicitly in the Hubbard Hamiltonian. Nevertheless electrostatic fields may arise from charge-density fluctuations in which the Coulomb interaction is not screened.

The continuum spin-orbit interaction may be written in terms of an SU(2) gauge field $\mathbf{A}_\mu$:

$$\mathcal{H}_{\text{spin orbit}} = \frac{\hbar}{2m}\mathbf{p}\cdot\mathbf{A}^\mu\sigma^\mu, \tag{3.4a}$$

where

$$\frac{\hbar}{2}\mathbf{A}^\mu\sigma^\mu = \frac{\hbar e}{2mc^2}\mathbf{E}\times\boldsymbol{\sigma} \tag{3.4b}$$

and the electric field $\mathbf{E}$ is the total microscopic electric field experienced by a given electron in the many-body system. In order to create a spin flux of π through an elementary plaquette, it is necessary that this electric field have a sufficient magnitude to probe the relativistic structure of the electron wave packet. Such electric fields arise from highly improbable quantum fluctuations. Accordingly, the rate of homogeneous spin-flux nucleation, by this mechanism, is many, many orders of magnitude slower than the rate of other electronic processes in the many-body system. The interaction Hamiltonian (3.4) nevertheless has the required symmetry to trigger a tunneling process between the periodic and antiperiodic sectors of the generalized Hilbert space. Heterogeneous nucleation near impurity potentials may increase the tunneling rate.

Unlike the physical electromagnetic field, the configurations of our SU(2) gauge field take the form of small quantized (in units of π) vortex loops in three dimensions. They can be nucleated by local electromagnetic and spin-orbit effects. When such a vortex loop (with a radius larger then lattice constant) penetrates the two-dimensional plane, it corresponds to the nucleation of a soliton-antisoliton pair. The structure of these solitons is described in Sec. IV. The dynamics of the SU(2) gauge field is determined entirely by the energetics of the many-electron system as specified by the Hubbard model interaction parameters. It is simply a mathematical device which implements our fundamental hypothesis of Sec. II. This is the conjecture that the many-electron Hilbert

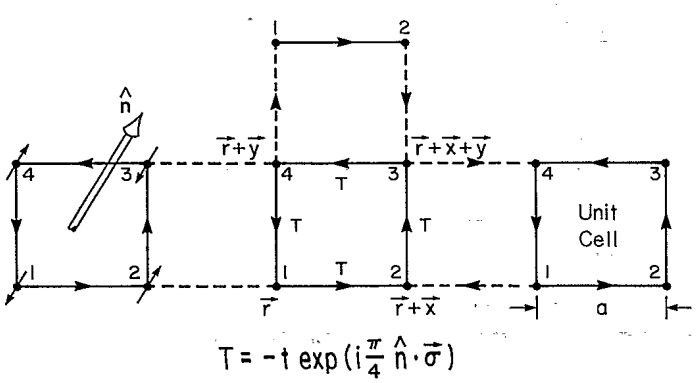

FIG. 4. Unit cell with a four-point basis. The spin-flux phase is obtained by associating the SU(2) matrix T (see text) with each directed link of the 2D lattice. Here $\mathbf{x} = a\hat{x}$ and $\mathbf{y} = a\hat{y}$. The vector $\hat{n}$ is associated with each plaquette and describes the quantization axis for antiferromagnetic ordering ($\pm\hat{n}$) of the spin-$\frac{1}{2}$ moments on sites $1,\ldots,4$. These local moments are depicted by small arrows on the lattice sites.

space can be consistently extended to include both periodic as well as antiperiodic states and that both sectors are physically accessible. We emphasize that this effect is a many-body effect. For a single electron, a transition between the periodic and antiperiodic sectors of the extended Hilbert space is forbidden by angular momentum conservation. It would require that a half-unit ($\hbar/2$) of angular momentum be added or removed in the process. The vortex loop in the many-electron system, however, penetrates the lattice in two places. Therefore, the creation of a soliton-antisoliton pair requires only integral units of total angular momentum to be exchanged with the physical electromagnetic field.

We consider a general Hartree-Fock, mean-field, factorization[16,28] of the Hubbard model in which the ground state expectation value of the electron spin operator is given by $\frac{1}{2}\langle c^\dagger_{i\alpha}\boldsymbol{\sigma}^{\alpha\beta}c_{i\beta}\rangle = s\hat{n}_i$, where $\hat{n}_i = \pm\hat{n}(\mathbf{r})$ is a unit vector describing the orientation of the local magnetic moment at each lattice site i, and $\hat{n}(\mathbf{r})$ is a slowly varying plaquette variable which defines the axis of quantization of the local antiferromagnetic ordering. For the uniform antiferromagnet one can choose $\hat{n}(\mathbf{r}) = +\hat{z}$. [Later, we will introduce magnetic textures by allowing $\hat{n}(\mathbf{r})$ to vary slowly with $\mathbf{r}$.]

A simple topological variant of this spin-density-wave state may now be obtained by associating the SU(2) matrix $T \equiv -t\exp\{i\frac{\pi}{4}[\hat{n}(\mathbf{r})\cdot\boldsymbol{\sigma}]\}$ with each directed link of the lattice as depicted in Fig. 4. With this choice it is apparent that the product of SU(2) matrices around any elementary plaquette of the 2D square lattice is equal to -1.

In the topological sector defined in Fig. 4, the unit cell now contains four lattice sites labeled $j = 1,\ldots,4$, and accordingly we define a set of four two-component spinor fields $\chi^{\dagger(j)} \equiv (c^\dagger_{j\uparrow}, c^\dagger_{j\downarrow})$ to describe the one-electron wave function. The kinetic energy term of the Hubbard Hamiltonian may be expressed in terms of these spinors as

$$\begin{aligned}\mathrm{KE} &\equiv \sum_{\langle ij\rangle}\left[c^\dagger_{i\alpha}T^{ij}_{\alpha\beta}c_{j\beta} + \mathrm{H.c.}\right] \\ &= \sum_{\mathbf{r}}\{\chi^{\dagger(2)}_{\mathbf{r}+\hat{x}a}T\chi^{(1)}_{\mathbf{r}} + \chi^{\dagger(2)}_{\mathbf{r}-a\hat{x}}T\chi^{(1)}_{\mathbf{r}} + \chi^{\dagger(3)}_{\mathbf{r}+a\hat{x}+a\hat{y}}T\chi^{(2)}_{\mathbf{r}+a\hat{x}} + \chi^{\dagger(3)}_{\mathbf{r}+a\hat{x}-a\hat{y}}T\chi^{(2)}_{\mathbf{r}+a\hat{x}} + \chi^{\dagger(4)}_{\mathbf{r}+a\hat{y}}T\chi^{(3)}_{\mathbf{r}+a\hat{x}+a\hat{y}} + \chi^{\dagger(4)}_{\mathbf{r}+2a\hat{x}+a\hat{y}}T\chi^{(3)}_{\mathbf{r}+a\hat{x}+a\hat{y}} \\ &\quad + \chi^{\dagger(1)}_{\mathbf{r}}T\chi^{(4)}_{\mathbf{r}+a\hat{y}} + \chi^{\dagger(1)}_{\mathbf{r}+2a\hat{y}}T\chi^{(4)}_{\mathbf{r}+a\hat{y}}\} + \mathrm{H.c.}\end{aligned} \tag{3.5}$$

Here, the subscript on χ denotes the actual location of the site in question and the summation over $\mathbf{r}$ is a summation over plaquettes. It is convenient to introduce the Fourier transform $\chi^{(j)}_{\mathbf{k}}$ defined by

$$\chi^{(j)}_{\mathbf{r}} = N^{-1/2}\sum_{\mathbf{k}} e^{i\mathbf{k}\cdot\mathbf{r}}\chi^{(j)}_{\mathbf{k}} \ . \tag{3.6}$$

Here, N is the number of plaquettes in the lattice and the summation over $\mathbf{k}$ extends over the reduced Brillouin zone depicted in Fig. 5. The mean-field Hamiltonian can now be expressed in terms of an eight-component field $\Psi^\dagger(\mathbf{r}) \equiv (\chi^{\dagger(1)}, \chi^{\dagger(2)}, \chi^{\dagger(3)}, \chi^{\dagger(4)})$ defined on the plaquette containing $\mathbf{r}$. In terms of the lattice Fourier transform $\Psi_{\mathbf{k}}$, the kinetic energy may be compactly re-expressed as

$$\mathrm{KE} = \sum_{\mathbf{k}} \Psi^\dagger_{\mathbf{k}}[A_x(\mathbf{k}) + A_y(\mathbf{k})]\Psi_{\mathbf{k}}, \tag{3.7a}$$

where the 8×8 matrices describing hopping in the x and y directions, respectively, are given by

$$A_x(\mathbf{k}) = 2\cos(k_x a)\begin{bmatrix} 0 & T^\dagger & 0 & 0 \\ T & 0 & 0 & 0 \\ 0 & 0 & 0 & T^\dagger \\ 0 & 0 & T & 0 \end{bmatrix} \tag{3.7b}$$

and

$$A_y(\mathbf{k}) = 2\cos(k_y a)\begin{bmatrix} 0 & 0 & 0 & T \\ 0 & 0 & T^\dagger & 0 \\ 0 & T & 0 & 0 \\ T^\dagger & 0 & 0 & 0 \end{bmatrix} . \tag{3.7c}$$

An interesting feature of the uniform spin-flux phase is that these matrices anticommute:

$$\{A_x(\mathbf{k}), A_y(\mathbf{k})\} = 0 \ . \tag{3.8}$$

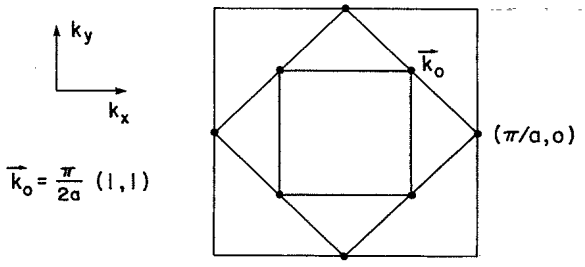

FIG. 5. Reduced Brillouin zone (inner square) for the spin-flux phase. Here, a is the lattice constant. The large square is the Brillouin zone of a free-electron gas. The middle square defines the band edge for a conventional antiferromagnet with one electron per site. The point $\mathbf{k}_0$ and its symmetry related partners define the band edge for the corresponding topological antiferromagnet. A "relativistic" continuum Hamiltonian is obtained by linearizing the dispersion relation about these four zone-corner points.

This is a direct consequence of the topological phase factor acquired by the electron as it encircles an elementary plaquette. As we will see, this anticommutation algebra between hopping in the x and y directions is a necessary and sufficient condition to provide a quasirelativistic dispersion relation for single-particle excitations. Rather than the conventional anisotropic dispersion relation of electrons on a two-dimensional square lattice which takes the form $\epsilon_{\mathbf{k}} = -2t[\cos(k_x a) + \cos(k_y a)]$, the dispersion relation in the presence of spin flux becomes $\epsilon_{\mathbf{k}} = \pm 2t[\cos^2(k_x a) + \cos^2(k_y a)]^{1/2}$. This is a simple illustration of the fundamental connection between topology, relativity, spin, and statistics.[35] In addition to the usual Pauli matrices $\boldsymbol{\sigma}$, which act on the internal spin space of the electron, it is convenient to introduce two new sets of 4×4 matrices which act on the four site indices of the elementary unit cell:

$$\boldsymbol{\tau} = \begin{bmatrix} \boldsymbol{\sigma} & 0 \\ 0 & \boldsymbol{\sigma} \end{bmatrix} \tag{3.9a}$$

and

$$\gamma_z \equiv \begin{bmatrix} I & 0 \\ 0 & -I \end{bmatrix}, \quad \gamma_y = i \begin{bmatrix} 0 & -I \\ I & 0 \end{bmatrix}, \quad \gamma_x = \begin{bmatrix} 0 & I \\ I & 0 \end{bmatrix}. \tag{3.9b}$$

Clearly, the set $\boldsymbol{\tau}$ and the set $\boldsymbol{\gamma}$ individually satisfy a cyclic Pauli spin algebra, but commute with each other: $[\tau_j, \gamma_k] = 0$ for all j and k. Using the direct tensor product of these matrices with the physical Pauli spin matrices $\boldsymbol{\sigma}$ (which act on the electron's *internal* wave function), it is possible to rewrite the kinetic energy term of the Hubbard Hamiltonian in the 8×8 matrix form

$$\mathcal{H}_0 \equiv -2t \sum_{\mathbf{k}} \Psi_{\mathbf{k}}^{\dagger} [\cos(k_x a)\tilde{\alpha}_x + \cos(k_y a)\tilde{\alpha}_y] \Psi_{\mathbf{k}} \ , \tag{3.10}$$

where

$$\begin{aligned} \tilde{\alpha}_x &\equiv [\tau_x + (\hat{n} \cdot \boldsymbol{\sigma})\tau_y]/\sqrt{2} \ , \\ \tilde{\alpha}_y &\equiv [\tau_x - (\hat{n} \cdot \boldsymbol{\sigma})\tau_y]\gamma_x/\sqrt{2}, \end{aligned} \tag{3.11}$$

and $\Psi_{\mathbf{k}} \equiv (N)^{-1/2} \sum_{\mathbf{r}_i} e^{-i\mathbf{k}\cdot\mathbf{r}_i} \Psi(\mathbf{r}_i)$. Here a is the lattice constant, N is the number of unit cells, and the reduced Brillouin zone for the $\mathbf{k}$ summation is $|k_x|, |k_y| < \pi/2a$. Similarly, the antiferromagnetic mean-field interaction term $U \sum_i c_i^{\dagger\alpha} \langle \mathbf{s}_i \rangle \cdot \boldsymbol{\sigma}_{\alpha\beta} c_i^{\beta}$ becomes

$$\mathcal{H}_{\text{int}}^{\text{MF}} \equiv -m \sum_k \Psi_k^{\dagger} (\tilde{\alpha}_z \gamma_x) \Psi_k, \tag{3.12}$$

where $\tilde{\alpha}_z \equiv -(\hat{n} \cdot \boldsymbol{\sigma})\tau_z \gamma_x$ and $m \equiv U|\langle \mathbf{s}_i \rangle|$ defines the magnitude of the antiferromagnetic, Mott-Hubbard gap. We remind the reader that the unit vector $\hat{n}$ is a plaquette variable and not a site variable associated with local moment orientation. For the antiferromagnet, the site localized moments are $\pm s\hat{n}$. This sign alternation within a plaquette is contained entirely in the structure of the 4×4 matrix τ_z.

A straightforward calculation reveals that the 8×8 matrices $\boldsymbol{\alpha} \equiv (\tilde{\alpha}_x, \tilde{\alpha}_y, \tilde{\alpha}_z)$ themselves satisfy a cyclic Pauli spin algebra with $\{\tilde{\alpha}_i, \tilde{\alpha}_j\} = 2\delta_{ij}$. This implies that the single-electron spectrum for the topological antiferromagnet at mean-field level has the relativistic, Dirac form $E = \pm\sqrt{4t^2[\cos^2(k_x a) + \cos^2(k_y a)] + m^2}$. The band edges for the lower and upper Mott-Hubbard bands occur at the four equivalent zone-corner points $\mathbf{k}_0 = (\pi/2a)(\pm 1, \pm 1)$. An effective, one-electron, continuum Hamiltonian may be obtained by linearizing the dispersion relation about these points and making the replacement $\mathbf{k} - \mathbf{k}_0 \to -i\boldsymbol{\nabla} \equiv -i(\partial_x, \partial_y)$:

$$\mathcal{H}_{\text{eff}} = 2ita(\tilde{\alpha}_x \partial_x + \tilde{\alpha}_y \partial_y) - m\tilde{\alpha}_z \gamma_x \ . \tag{3.13}$$

This effective one-electron Hamiltonian is an exact mapping of the antiferromagnetic spin-flux state of the Hubbard model to a (2+1)-dimensional, relativistic, Dirac field theory with "charge conjugation symmetry." In addition to the complete anticommutation algebra of the matrices $\tilde{\alpha}_x, \tilde{\alpha}_y$ and $\tilde{\alpha}_z \gamma_x$, the matrix $\tilde{\alpha}_c \equiv \tilde{\alpha}_y \gamma_y$ anticommutes with $\mathcal{H}_{\text{eff}}$. This guarantees that the spectrum of $\mathcal{H}_{\text{eff}}$ is symmetric about $E = 0$. We also note that the operator γ_x is a constant of motion since $[\mathcal{H}_{\text{eff}}, \gamma_x] = 0$. This is associated with a sublattice degeneracy of the 2D square lattice. The "mass" parameter $m \equiv U|\langle \mathbf{s}_i \rangle|$ must be determined by a self-consistent Hartree-Fock calculation as in the case of conventional spin-density-wave theory. A detailed evaluation of the mean-field (Hartree-Fock) energy of the spin-flux state as a function of the microscopic interaction parameter U/t, doping δ, next-nearest neighbors and interlayer coupling will be presented elsewhere. This will determine the region of the mean-field phase diagram in which the spin flux is energetically favored over conventional spiral magnetic states. We believe, however, that the true energetics of the many-body system is dominated by fluctuation corrections to mean-field theory. Fluctuations may be incorporated into the effective Hamiltonian (3.13) through the factor of $\hat{n}(\mathbf{r}) \cdot \boldsymbol{\sigma}$ which enters each of the matrices $\tilde{\alpha}_x, \tilde{\alpha}_y$, and $\tilde{\alpha}_z$. If the plaquette orientation vector $\hat{n}(\mathbf{r})$ is allowed to rotate slowly from point to point in space, this corresponds to slowly varying twist of the local moment background, while maintaining antiferromagnetic correlation within a given plaquette. [In a path-integral representation of the original Hubbard model, the matrix field $\hat{n}(\mathbf{r}) \cdot \boldsymbol{\sigma}$ would emerge as a Hubbard-Stratonovitch decoupling field for the Hubbard interaction and acquire a dynamics of its own.[16–18]] The experimental observation of spin-liquid behavior of the doped copper-oxide materials[3] suggests that the true physics of the many-electron system is not determined by the Hartree-Fock energy and band structure of either the conventional spiral magnetic states or the uniform spin-flux phase alone but rather by localized tunneling events between these two mean-field states. We proceed, therefore, to a detailed investigation of the nature of magnetic soliton textures which give rise to such tunneling and the subgap electronic structure which they induce.

IV. TOPOLOGICAL MAGNETIC SOLITONS

In this section we describe the nature of magnetic textures which occur in the uniform topological antiferro-

magnet. Remarkably, the structure of these solitons is uniquely specified by geometry. We remind the reader that the occurrence of topological spin flux as well as the very existence of spin-$\frac{1}{2}$ electrons is a direct consequence of the geometry of physical three-dimensional space as embodied in the group manifold of SO(3). We demonstrate, in this section that the requirement that the continuum mean-field Hamiltonian (3.13) retains cylindrical (two-dimensional) symmetry in the presence of a magnetic texture completely specifies the form of this texture. This is the requirement that the z component of the total angular momentum in the many-body wave function remain a constant of motion. In terms of polar coordinates $\mathbf{r} = (r, \phi)$, it follows that the operators $\mathrm{H}_{\mathrm{eff}}$, γ_x, and $i\partial_\phi$ form complete set of commuting operators. The uniqueness of the magnetic soliton textures is further illustrated by the fact that the condition $[\mathrm{H}_{\mathrm{eff}}, i\partial_\phi] = 0$ is completely equivalent to the condition that the classical magnetic twist energy of the texture defined by the integral $\int d^2\mathbf{r}[\partial_\mu \hat{n}(\mathbf{r})]^2$ is a local minimum.

We emphasize that the results which we derive in this section refer to the topology of the spin flux phase, namely $\pi_1[\mathrm{SO}(3)]$. Analogous considerations have been applied by Wiegmann[36] and Khveshchenko and Wiegmann[37] to the earlier U(1) charge-flux phases.

Twist of the magnetic background away from antiferromagnetic alignment from one plaquette to another may be accomplished by allowing the matrices $\boldsymbol{\alpha}$ to have slow spatial variations through the factor $\hat{n}(\mathbf{r}) \cdot \boldsymbol{\sigma}$ which they contain. It is shown in Appendix B that the generalization of $\mathcal{H}_{\mathrm{eff}}$ for any magnetic texture which varies slowly on the scale of the lattice constant is obtained by symmetrizing the kinetic energy with respect to the momentum operator $\mathbf{p} \equiv -i\boldsymbol{\nabla}$. In particular the Hermiticity of $\mathcal{H}_{\mathrm{eff}}$ is preserved for spatially varying $\hat{n}(\mathbf{r})$ if we make the replacement $\boldsymbol{\alpha} \cdot \mathbf{p} \to \frac{1}{2}[\boldsymbol{\alpha} \cdot \mathbf{p} + \mathbf{p} \cdot \boldsymbol{\alpha}]$. These spatial variations, while preserving the symmetry of the eigenvalue spectrum of $\mathcal{H}_{\mathrm{eff}}$ about $E = 0$, give rise to localized electronic states within the relativistic Mott-Hubbard gap.

For the sake of argument we consider a uniform topological antiferromagnet which is polarized in the z direction, perpendicular to the x-y plane of the two-dimensional square lattice. In this case $\hat{n}(\mathbf{r}) = \hat{z}$ and the local moment structure within an elementary plaquette takes the form $\langle \mathbf{s}_i \rangle = \pm s\hat{n}(\mathbf{r})$. We now allow the plaquette variable $\hat{n}(\mathbf{r})$ to have slow spatial variations from one plaquette to the next. It is convenient to parametrize a general rotation of $\hat{n}(\mathbf{r})$ by means of the spatially varying unitary matrix $U(\mathbf{r})$:

$$\hat{n}(\mathbf{r}) \cdot \boldsymbol{\sigma} = U^\dagger(\mathbf{r})\sigma_z U(\mathbf{r}) \ . \tag{4.1}$$

The symmetrized, Hermitian, effective Hamiltonian (3.8) can be rewritten as

$$\mathcal{H}_{\mathrm{eff}} = ita\left[\{\tilde{\alpha}_x, \partial_x\} + \{\tilde{\alpha}_y, \partial_y\}\right] - m\tilde{\alpha}_z\gamma_x, \tag{4.2}$$

where the anticommutator $\{\tilde{\alpha}_x, \partial_x\} \equiv \tilde{\alpha}_x\partial_x + \partial_x\tilde{\alpha}_x$ signifies that the spatial derivatives act on *everything* to the right-hand side. Inserting the general magnetic texture, (4.1), into the matrices $\tilde{\alpha}_\mu$, $\mu = x, y, z$, we may rewrite

$$\mathcal{H}_{\mathrm{eff}} \equiv U^\dagger(\mathbf{r})\mathcal{H}U(\mathbf{r}), \tag{4.3a}$$

where

$$\mathcal{H} = 2ita[\alpha_x\partial_x + \alpha_y\partial_y + \tfrac{1}{2}V] + m\beta \ . \tag{4.3b}$$

Here

$$\alpha_x \equiv (\tau_x + \sigma_z\tau_y)/\sqrt{2}, \tag{4.4a}$$

$$\alpha_y \equiv (\tau_x - \sigma_z\tau_y)\gamma_x/\sqrt{2}, \tag{4.4b}$$

$$\beta \equiv -\alpha_z\gamma_x, \tag{4.4c}$$

$$\alpha_z \equiv -\sigma_z\tau_z\gamma_x \tag{4.4d}$$

are spatially nonvarying 8×8 matrices. The price that must be paid for removing spatial variations from the $\tilde{\alpha}$ matrices is the introduction of a new potential

$$V \equiv \{D_x, \alpha_x\} + \{D_y, \alpha_y\}, \tag{4.5a}$$

where the "invariant derivative" is defined as

$$D_\mu \equiv U(\mathbf{r})\partial_\mu U^\dagger(\mathbf{r}) \ . \tag{4.5b}$$

In deriving the transformed effective Hamiltonian (4.3b) we have made use of the fact that

$$\partial_\mu(U^\dagger U) = \partial_\mu(\mathbf{1}) = 0 \ .$$

The eigenvalue spectrum in the presence of a magnetic texture is determined by the Schrödinger equation $\mathcal{H}_{\mathrm{eff}}\psi_0(\mathbf{r}) = E\psi_0(\mathbf{r})$. In terms of the transformed, eight-component wave function $\psi_1(\mathbf{r}) \equiv U(\mathbf{r})\psi_0(\mathbf{r})$, this becomes

$$\mathcal{H}\psi_1 = E\psi_1 \tag{4.6}$$

with $\mathcal{H}$ given by (4.3b). Even in the presence of spatially varying magnetic textures the eigenvalue spectrum of (4.6) remains symmetric about $E = 0$. This follows from the observation that if $\psi_1(\mathbf{r})$ is a solution of (4.6) with energy E, then $\sigma_y\psi_1^*(\mathbf{r})$ is a solution with energy $-E$. To demonstrate this, we make use of the identities $\sigma_y\alpha_\mu^*\sigma_y = \alpha_\mu$ for $\mu = x, y$, $\sigma_y\beta^*\sigma_y = -\beta$ and $\sigma_y U^*(\mathbf{r})\sigma_y = U(\mathbf{r})$ for any unitary spin-rotation matrix. It follows that $\sigma_y\mathcal{H}^*\sigma_y = -\mathcal{H}$. Noting that $\sigma_y^2 = 1$, it follows from (4.6) that $\sigma_y\mathcal{H}^*\sigma_y^2\psi_1^* = E\sigma_y\psi_1^*$. Therefore,

$$\mathcal{H}(\sigma_y\psi_1^*) = -E(\sigma_y\psi_1^*) \tag{4.7}$$

as required.

We consider next a general axially symmetric configuration of the background field $\hat{n}(\mathbf{r})$ and transform (4.6) to polar coordinates $\mathbf{r} = (r\cos\phi, r\sin\phi)$. First we have to transform the kinetic energy term in (4.6)

$$\begin{aligned} i\alpha_x\partial_x + i\alpha_y\partial_y &= i\alpha_x\left(\cos\phi\partial_r - \frac{\sin\phi}{r}\partial_\phi\right) \\ &\quad + i\alpha_y\left(\sin\phi\partial_r + \frac{\cos\phi}{r}\partial_\phi\right) \\ &= i(\alpha_x\cos\phi + \alpha_y\sin\phi)\partial_r \\ &\quad + i(\alpha_y\cos\phi - \alpha_x\sin\phi)\frac{\partial_\phi}{r} \ . \end{aligned} \tag{4.8}$$

Since the α matrices satisfy the cyclic algebra $\alpha_\mu\alpha_\nu = i\epsilon_{\mu\nu j}\alpha_j + \delta_{\mu\nu}$ it follows that

$$(\alpha_x \cos\phi + \alpha_y \sin\phi) = \alpha_x \exp(i\alpha_z\phi) \tag{4.9}$$

and

$$(\alpha_y \cos\phi + \alpha_x \sin\phi) = \alpha_y \exp(i\alpha_z\phi). \tag{4.10}$$

Therefore,

$$i\alpha_x\partial_x + i\alpha_y\partial_y$$

$$= \exp(-i\alpha_z\phi/2)\left[i\alpha_x\left(\partial_r + \frac{1}{2r}\right) + i\alpha_y\frac{\partial_\phi}{r}\right] \times \exp(i\alpha_z\phi/2). \tag{4.11}$$

Thus, by means of the unitary transformation of the wave function $\psi_1(\mathbf{r}) \to \exp(i\alpha_z\phi/2)\psi_1(\mathbf{r})$ we can achieve the separation of variables in a free ($D_\mu = 0$) Dirac equation. Next we consider the transformation of the invariant derivatives term in (4.6) to the polar coordinates. We will take rotation $U(\mathbf{r})$ in the form compatible with the axial symmetry of the problem:

$$U(\mathbf{r}) = \exp[-i\sigma_y\theta(r)/2]\exp(i\mu\sigma_z\phi/2), \tag{4.12}$$

where $\theta(r)$ is a general function describing the magnetic twist in the radial direction and the integer parameter μ is a topological charge[38,39] of the $\hat{n}$ field provided that $\theta(r)$ varies from 0 to π while r runs from 0 to ∞. A detailed review of magnetic textures which are local minima of the classical magnetic twist energy, $\int d^2\mathbf{r}(\partial_\mu\hat{n})^2$, is given in Appendix C.

In polar coordinates, it is straightforward to verify that the invariant derivative potential V, Eq. (4.5a), may be rewritten as

$$V = \{D_r, \alpha_x e^{i\alpha_z\phi}\} + \frac{1}{r}\{D_\phi, \alpha_y e^{i\alpha_z\phi}\}, \tag{4.13}$$

where the radial and angular invariant derivatives D_r and D_ϕ are related to their Cartesian counterparts by

$$D_x = \cos\phi D_r - \frac{\sin\phi}{r}D_\phi \tag{4.14a}$$

and

$$D_y = \sin\phi D_r + \frac{\cos\phi}{r}D_\phi \ . \tag{4.14b}$$

Introducing the transformed invariant derivatives

$$\tilde{D}_\mu \equiv e^{i\alpha_z\phi/2}D_\mu e^{-i\alpha_z\phi/2} \ , \tag{4.15}$$

it follows that

$$V = e^{-i\alpha_z\phi/2}\tilde{V}e^{i\alpha_z\phi/2}, \tag{4.16a}$$

where

$$\tilde{V}(\mathbf{r}) \equiv \{\tilde{D}_r, \alpha_x\} + \frac{1}{r}\{\tilde{D}_\phi, \alpha_y\} \ . \tag{4.16b}$$

This is analogous to the free kinetic energy term (4.11). Defining the transformed wave function $\psi_2 \equiv \sqrt{r}e^{i\alpha_z\phi/2}U(\mathbf{r})\psi_0$, the Schrödinger equation (4.6) takes the form

$$\mathcal{H}\psi_2 = E\psi_2,$$

where

$$\mathcal{H} = 2ita\left(\alpha_x\partial_r + \frac{\alpha_y}{r}\partial_\phi + \frac{1}{2}\tilde{V}(\mathbf{r})\right) + m\beta. \tag{4.17}$$

The effects of the magnetic texture are completely contained in the potential $\tilde{V}(\mathbf{r})$. We wish to determine the conditions under which this potential is amenable to separation of variables in the polar coordinates r and ϕ. Accordingly, we evaluate $\tilde{V}(\mathbf{r})$ for the axially symmetric rotation field (4.12).

Using the representation of the α matrices (4.4), a straightforward but lengthy calculation gives [using (4.12)]

$$\tilde{V}(\mathbf{r}) = \frac{-i\mu}{r}\cos\theta(r)\sigma_z\alpha_y + \frac{i\tau_x}{\sqrt{2}}[\cos\phi A_-(r) + \sin\phi A_+(r)\gamma_x], \tag{4.18}$$

where

$$A_\pm(r) = \left((\partial_r\theta)\sigma_y \pm \frac{\mu}{r}\sin\theta\sigma_x\gamma_x\right)/\sqrt{2}. \tag{4.19}$$

Separation of variables in the Schrödinger equation is possible if there exists a unitary transformation which when applied to $\tilde{V}(\mathbf{r})$ leaves it independent of ϕ. This in turn is possible if the matrices defined by Eq. (4.19) anticommute. Explicitly,

$$\{A_+(r), A_-(r)\} = (\partial_r\theta)^2 - \frac{\mu^2}{r^2}\sin^2\theta \ . \tag{4.20}$$

Requiring that this vanish, yields the condition

$$\partial_r\theta = s_1\frac{\mu}{r}\sin\theta, s_1 = \pm 1 \tag{4.21}$$

on the radial function $\theta(r)$. Remarkably, this condition is mathematically equivalent (see Appendix C) to the requirement that the function $\theta(r)$ correspond to a local minimum of the classical magnetic twist energy:

$$\mathcal{H}_{\text{mag}} \equiv \int d^2\mathbf{r}(\partial_\mu\hat{n})\cdot(\partial_\mu\hat{n}) \ . \tag{4.22}$$

The separability condition (4.21) may also be arrived at by requiring that the product of SU(2) matrices $T^{12}T^{23}T^{34}T^{41}$ remains equal to -1 around all plaquettes (except the plaquette containing the soliton core) to leading order in the gradient expansion. In physical terms, the symmetrization procedure (derived in Appendix B) for the kinetic energy, allows relaxation of the orientation of local moments *within* a given plaquette in response to the formation of a magnetic texture. The auxiliary condition (4.21) is therefore necessary to preserve the flux quantization requirement in the presence of this *internal*

relaxation.

Using the condition (4.21) we may now derive a purely radial Schrödinger equation. For this purpose it is convenient to define the spatially nonvarying matrices

$$\tilde{A}_{\pm} = (\sigma_y \pm s_1 \gamma_x \sigma_x)/\sqrt{2}. \tag{4.23}$$

Clearly, $A_{\pm} = \partial_r \theta \tilde{A}_{\pm}$ with $\{\tilde{A}_+, \tilde{A}_-\} = 0$. Also, $\tilde{A}_+, \tilde{A}_-$, and $s_1 \sigma_z \gamma_x$ satisfy a cyclic Pauli algebra. It follows that

$$\tilde{V}(\mathbf{r}) = -i\frac{\mu}{r}\cos\theta \sigma_z \alpha_y + \frac{i\tau_x}{\sqrt{2}}\partial_r \theta e^{is_1\sigma_z\phi/2}\tilde{A}_- e^{-is_1\sigma_z\phi/2}. \tag{4.24}$$

Using the fact that σ_z commutes with τ_x, α_x, and α_y, we obtain an equation for the transformed wave function $\psi_3 \equiv \sqrt{r} e^{-is_1\sigma_z\phi/2} e^{-i\alpha_z\phi/2} U \psi_0$:

$$\mathcal{H}\psi_3 = E\psi_3, \tag{4.25a}$$

where

$$\mathcal{H} = 2ita\left[\alpha_x\partial_r + \frac{\alpha_y}{r}(\partial_\phi + is_1\sigma_z/2)\right] + m\beta - t\frac{a\mu}{r}[s_1 \sin\theta(r)\tau_x\tilde{A}_- - \cos\theta(r)\sigma_z\alpha_y]. \tag{4.25b}$$

This effective Hamiltonian clearly has no explicit dependence on ϕ. Since $[i\partial_\phi, \mathcal{H}] = 0$, a purely radial Schrödinger equation may be obtained by replacing $i\partial_\phi$ by an angular momentum quantum number ℓ. Before doing this, we make some final simplifications in the matrix structure using the identities

$$\begin{aligned} \tilde{A}_- &= e^{-is_1\gamma_x\sigma_x\pi/8}\sigma_y e^{is_1\gamma_x\sigma_x\pi/8}, \\ \alpha_x &= e^{-i\sigma_z\tau_z\pi/8}\tau_x e^{i\sigma_z\tau_z\pi/8}, \\ \alpha_y &= e^{-i\sigma_z\tau_z\pi/8}(-\gamma_x\sigma_z\tau_y)e^{i\sigma_z\tau_z\pi/8}. \end{aligned} \tag{4.26}$$

Applying the unitary transformation defined by $\psi_4 = e^{i\sigma_z\tau_z\pi/8}e^{is_1\gamma_x\sigma_x\pi/8}\psi_3$, (4.25) becomes

$$\mathcal{H}\psi_4 = E\psi_4 \ . \tag{4.27a}$$

Here

$$\mathcal{H} = 2ita\left[\tau_x\partial_r - \frac{\gamma_x}{r}\sigma_z\tau_y\left(\partial_\phi + i\frac{s_1}{2}\sigma_z\right)\right] + m\beta - t\frac{a\mu}{r}[s_1\sin\theta\tau_x\sigma_y + \cos\theta\gamma_x\tau_y] \ . \tag{4.27b}$$

It is straightforward to verify that $\mathcal{H}$, $i\partial_\phi$, and γ_x constitute a complete set of commuting operators. In addition to the angular momentum quantum number ℓ, we denote the eigenvalues of γ_x by $s_2 = \pm 1$. In Appendix C we describe in detail our method for solving this radial Schrödinger equation. A summary of the results is presented in Figs. 7—9.

The general solution of Eq. (4.21) takes the form (see Appendix C)

$$\theta(r) = 2\tan^{-1}(r/\rho_c)^{\mu s_1},$$

where ρ_c is an arbitrary scale parameter which defines the core radius of the soliton. The $\mu = 1$ soliton is depicted in Fig. 6. The validity of the continuum approximation, however, requires that $\rho_c \geq a$. For all nonzero values of μ, the soliton texture induces localized one-electron states within the Mott-Hubbard gap. For a very large core radius $\rho_c \gg a$, there are in general a number of angular momentum states labeled by the quantum number ℓ. Each state is doubly degenerate. This degeneracy corresponds to an electronic wave function which resides primarily on one sublattice of the underlying 2D square lattice and its partner which resides primarily on the other sublattice. The sublattice electronic probability density for an $\ell = 1/2$ angular momentum state in the $\mu = 1$ Skyrmion texture is depicted in Fig. 9. This broken sublattice symmetry is invariably a consequence of the on-site Hubbard repulsion, which prevents a degenerate pair of localized electrons from occupying the same sites. For any given state of energy E and angular momentum ℓ, there is a corresponding state of energy $-E$ and angular momentum $-\ell$. The symmetries and degeneracies of the soliton spectrum are summarized in Table I. For all solitons, both integer and half-integer values of ℓ are considered since we have allowed both periodic and antiperiodic wave functions within the extended Hilbert space. However, as the soliton core size ρ_c shrinks to the scale of the lattice constant a, high angular momentum states merge into the Mott-Hubbard continuum, leaving behind only a few low-ℓ states within the gap.

For a Skyrmion texture with topological charge $\mu = 1$, it is necessary that $\ell \neq 0$ for the physical wave function to be nonsingular at the origin (see Appendix C). Setting $s_1 = 1$ and $\ell = 1/2$ yields the solid curve in Fig. 7.

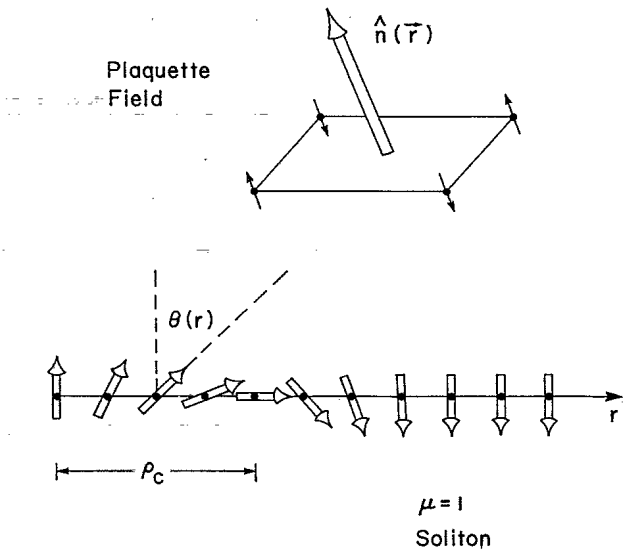

FIG. 6. The radial dependence of the plaquette vector field $\hat{n}(\mathbf{r})$ along a line passing through the center of a $\mu = 1$ hedgehog Skyrmion located at $\mathbf{r} = 0$. In polar coordinates $\mathbf{r} = (r, \phi)$, the vector field $\hat{n}(\mathbf{r})$ undergoes a 2π-vortex rotation as $\phi \to \phi + 2\pi$. Local antiferromagnetic order is inverted near the center of the soliton. The soliton core radius is denoted by ρ_c.

TABLE I. Symmetries and degeneracies in the subgap spectrum of localized, electronic states in the vicinity of a topological, magnetic soliton. Each energy level E is doubly degenerate. The associated wave functions break the A, B sublattice symmetry of the square lattice. If the wave function associated with quantum numbers (E, ℓ, s_2) resides primarily on sublattice A, the degenerate state $(E, -\ell, -s_2)$ resides primarily on sublattice B. Also, the spectrum is symmetric about $E = 0$. For any state (E, ℓ, s_2) there is a corresponding state with quantum numbers $(-E, -\ell, s_2)$.

$s_2 = +1$	$s_2 = -1$
E,l	$E,-l$
$-E,-l$	$-E,l$

The bound state (doublet) moves deeper into the Mott-Hubbard gap as the core radius ρ_c shrinks, reaching a minimum value of approximately 0.75 the midgap energy. The angular momentum quantum number ℓ refers to the transformed wave function $\psi_3(\mathbf{r})$. In order to determine the angular momentum of the physical wave function we must determine the transformation properties (under rotation) of the original wave function

$$\psi_0(\mathbf{r}) = e^{-is_1\gamma_z\pi/8} e^{is_1\sigma_z\phi/2} e^{-i\alpha_z\phi/2} U^\dagger(\mathbf{r})\psi_3(\mathbf{r}) \ .$$

For a $\mu = 1$ soliton, the matrix $U^\dagger(\mathbf{r})$ changes sign when $\phi \to \phi + 2\pi$. Therefore if $\psi_3(\mathbf{r})$ is an $\ell = 1/2$ state, the original wave function $\psi_0(\mathbf{r})$ transforms under rotations in the same way as states in the (topological) Dirac continuum. Like states in the Dirac continuum, this state is antiperiodic. On the other hand, the $\ell = 1$ state transforms under rotations like continuum states in the nontopological antiferromagnet and is not accessible from the Dirac continuum. The appearance of the periodic state is related to the fact that the $\mu = 1$ soliton induces an elementary unit of vorticity in the background magnetic moments and can be regarded as carrying a spin flux of π in its core. When added to the original spin flux of π that penetrates each plaquette it leads to a topologically trivial flux configuration. If solitons are free to move within the two-dimensional lattice, then the creation operator for a soliton at $\mathbf{r}$

$$V^\dagger(\mathbf{r}) = \exp\left(-i\mu \sum_j \hat{s}_j^z \phi_j(\mathbf{r})\right) \exp\left(-i \sum_j \hat{s}_j^y \theta_j(\mathbf{r})\right)$$

has the property that $R^z_{\rm ext} V^\dagger(\mathbf{r}) R^z_{\rm ext} = (-1)^\mu V^\dagger(\mathbf{r})$. Here, $\hat{s}_j^z$ and $\hat{s}_j^y$ are spin operators at lattice site j, $\phi_j(\mathbf{r})$ is the angle of the line connecting site j with the point $\mathbf{r}$, $\theta_j(\mathbf{r}) \equiv \theta(|\mathbf{r}_j - \mathbf{r}|)$ and the summation is over all sites on the square lattice. $R^z_{\rm ext}$ (as introduced in Sec. II) is an operator that performs a coordinate rotation of 2π about an axis $\hat{z}$ which passes through the vortex core $\mathbf{r}$. The one-electron transition from a periodic to an antiperiodic state which is now allowed by motion of the soliton vortex through the point $\mathbf{r}$ involves macroscopic phase rearrangement of all other electrons in the many-body system.

For topological charge $\mu = 2$, a nonsingular subgap wave function may be obtained by setting $s_1 = 1$ and $\ell = 0$. The bound state energies are shown in Fig. 8. The $\ell = 0$ state decreases monotonically with decreasing ρ_c, approaching a limiting value of approximately 0.64 of the midgap as $\rho_c \to 0$.

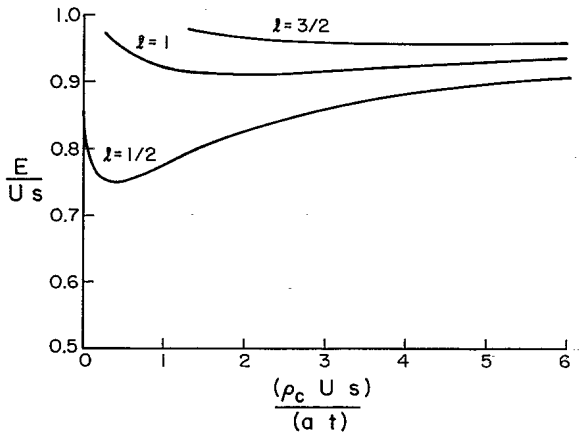

FIG. 7. Eigenvalue spectrum of the $\mu = 1$ hedgehog Skrymion plotted as a function of the dimensionless core radius parameter $x \equiv (\rho_c/a)(Us/t)$. $E = 0$ corresponds to the center of the "relativistic" Mott-Hubbard gap and $E = 1$ is the upper band edge. Each eigenvalue is doubly degenerate and the entire spectrum is symmetric about $E = 0$. The deepest state has quantum number $\ell = \frac{1}{2}$ and corresponds to an antiperiodic, physical state localized around the Skyrmion core. This state reaches a minimum energy of about $0.75Us$ when $x \simeq 0.4$. Higher angular momentum states appear as ρ_c increases.

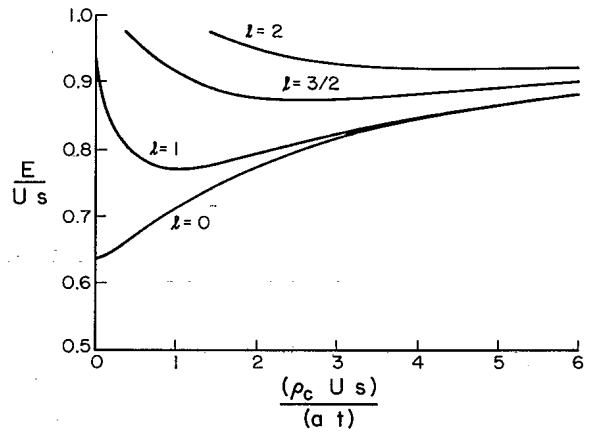

FIG. 8. Eigenvalue spectrum of the $\mu = 2$ soliton. The soliton corresponds to two coverings of the sphere S_2 by the plaquette field $\hat{n}(\mathbf{r})$. However, the internal Euler angle field of electrons which constitute this magnetic texture, crosses the surface (Fig. 1) of SO(3) twice. As a result it is not topologically stable on a lattice. The deepest localized electronic state has angular momentum quantum number $\ell = 0$.

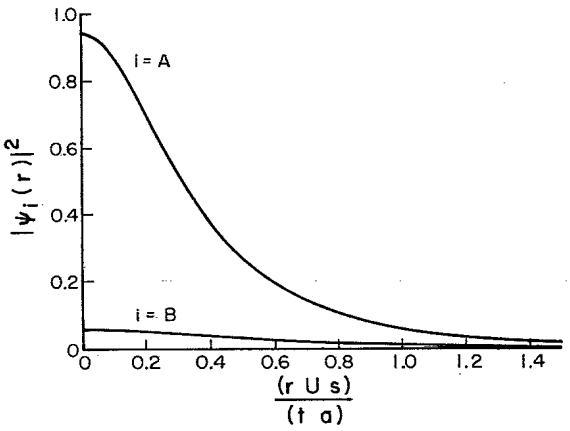

FIG. 9. Sublattice probability densities as a function of radius for the $\ell = \frac{1}{2}$ localized wave function, near the core of the $\mu = 1$ Skyrmion. The $\ell = \frac{1}{2}$ state is doubly degenerate. For one member of the degenerate pair, the wave function resides primarily on sublattice A with a smaller component on sublattice B. For the other member, the sublattice probability densities are interchanged. The soliton core radius ρ_c is indicated.

V. SUMMARY AND DISCUSSION

We have proposed an extension of the physical Hilbert space for an interacting many-body system consisting of spin-$\frac{1}{2}$ particles. This extension arises from the inherent two-valued nature of spin-$\frac{1}{2}$ wave functions. A pictorial representation of this extension follows from associating a Mobius strip with a closed electron trajectory which encircles an elementary plaquette of the two-dimensional lattice. Associate one value, χ, of the spinor wave function with one side of the Mobius strip and the other value, $-\chi$, with the other side. As the electron encircles the closed loop, the value of its wave function switches from one side of the strip to the other. In other words, the wave function is antiperiodic around the lattice plaquette. This π twist of the Mobius strip is mathematically equivalent to passing a *spin flux* of π through the plaquette. The SU(2) gauge field which describes this spin flux *does not* correspond to the addition of any external dynamical field despite the fact that the curl of this gauge field is nonzero. We suggest, however, that it *does* correspond to a new topological sector of Hilbert space for spin-$\frac{1}{2}$ electrons. This spin flux phase is distinct from previously discussed charge-flux phases.[30] Unlike the charge-flux state, the electrical currents associated with spin flux circulate in opposite directions for opposite components of spin, leading to no net physical magnetic field.

We have suggested that antiperiodicity of one-electron spinor states may arise in a strongly interacting electron gas in which the motion of an electron is strongly influenced by its interaction with the local magnetic moment background of the other electrons. Elementary units of spin flux may arise from vorticity in the local moment background. From purely geometrical considerations, we demonstrated that this vorticity is carried by hedgehog-Skyrmion, magnetic, textures. While Skyrmion textures may arise within the conventional (nontopological) antiferromagnet, their mathematical description is greatly facilitated by considering the alternative mean-field ground state into which they cause tunneling. This new mean-field state is a uniform (topological), spin flux, antiferromagnet. This state exhibits a quasirelativistic Mott-Hubbard band structure. The true ground state of a doped Mott-Hubbard electron system may in fact be described by a large number of local tunnelling events (solitons) between these two mean-field states. This quantum liquid of solitons may be responsible for the destruction of magnetic long range order with doping in the high-T_c oxide superconductors. Since the time scale of magnetic fluctuations is long compared to optical excitation time scales (across the Mott-Hubbard pseudogap), it is plausible that a well-defined subgap electronic structure exists even within a spin-liquid phase. This subgap electronic structure is associated with electronic wave functions localized near the core of a magnetic soliton. These localized states exhibit a variety of angular momentum quantum numbers including electric dipole allowed transitions which may lie in the midinfrared. Since magnetic solitons are strongly coupled to other fluctuations such as conventional spin waves, the spin-charge collective modes,[17] and other solitons, it is likely that electronic excitations within a given soliton are strongly damped. This provides a possible scenario for the ubiquitous, broadband, midinfrared optical absorption observed in copper-oxide superconductors.[40–42]

We emphasize that our magnetic solitons, although superficially similar to those which arise in semiclassical nonlinear σ models such as (4.22), in fact describe transitions to an entirely new type of wave function for spin-$\frac{1}{2}$ electrons. Accordingly they are associated with a generalized Hilbert space. This possibility is a very fundamental one which must be traced back to the formulation of quantum mechanics for spin-$\frac{1}{2}$ particles. Unlike the *variational* wave functions which describe fractional charge and fractional statistics of quasiparticles in the quantum Hall effect,[43] our states are those of the bare electrons themselves. Also, our antiperiodic (Mobius strip) wave functions are not a consequence of two-dimensionality but rather a consequence of the inherent two-valuedness of spin-$\frac{1}{2}$ wave functions. We hope that these considerations may provide some new avenues for understanding the unconventional properties of strongly interacting electron systems.

ACKNOWLEDGMENTS

S.J. would like to thank P. W. Anderson, G. Baskaran, and M. H. Cohen for some valuable discussions. This work was supported in part by the Natural Sciences and Engineering Research Council of Canada, the Canadian Institute of Advanced Research Program in Superconductivity, and the Ontario Laser and Lightwave Research Centre.

APPENDIX A: TOPOLOGY OF SPIN-$\frac{1}{2}$ WAVE FUNCTIONS

In this appendix we provide a brief review of the connection between the geometry of rotations in three-dimensional space and the two-valued *internal* wave function of spin-$\frac{1}{2}$ electrons. In general quantum mechanics is formulated from an underlying classical theory defined by a set of coordinates, conjugate momenta and a Lagrangian. Quantum mechanics is derived from the underlying classical mechanics by replacing the coordinates and the conjugate momenta by noncommuting operators. For the case of spin $\frac{1}{2}$, the underlying classical mechanics is that of the symmetric spinning top[11,12] described by a set of Euler angles $\boldsymbol{\eta} \equiv (\eta_1, \eta_2, \eta_3)$. In a space-fixed coordinate system (x, y, z), the components of angular velocity $\boldsymbol{\omega}$ are given by[13]

$$\begin{aligned} \omega_x &= \dot{\eta}_1 \cos\eta_2 + \dot{\eta}_3 \sin\eta_1 \sin\eta_2, \\ \omega_y &= \dot{\eta}_1 \sin\eta_2 - \dot{\eta}_3 \sin\eta_1 \cos\eta_2, \\ \omega_z &= \dot{\eta}_3 \cos\eta_1 + \dot{\eta}_2 \ . \end{aligned} \tag{A1}$$

For a symmetric, spinning top with moment of inertia I, the Lagrangian $\mathcal{L} = \frac{1}{2} I(\boldsymbol{\omega})^2$ is given by

$$\mathcal{L} = \frac{I}{2}(\dot{\eta}_1^2 + \dot{\eta}_2^2 + \dot{\eta}_3^2 + 2\dot{\eta}_2\dot{\eta}_3 \cos\eta_1) \ .$$

This may be regarded as the Lagrangian for free particle motion in a curved space [the group manifold of SO(3)] whose metric tensor[12] is given by $g_{11} = g_{22} = g_{33} = 1$ and $g_{23} = \cos\eta_1$. This is depicted in Fig. 1.

The conjugate momenta, $p_i \equiv \frac{\partial \mathcal{L}}{\partial \dot{\eta}_i}$, are given by

$$\begin{aligned} p_1 &= I\dot{\eta}_1, \\ p_2 &= I(\dot{\eta}_2 + \dot{\eta}_3 \cos\eta_1), \\ p_3 &= I(\dot{\eta}_3 + \dot{\eta}_2 \cos\eta_1) \ . \end{aligned} \tag{A2}$$

The Hamiltonian, $\mathcal{H} = \sum_i \dot{\eta}_i p_i - \mathcal{L}$, may be expressed in terms of this conjugate momenta:

$$\mathcal{H} = \frac{1}{2I}\left\{p_1^2 + \frac{1}{\sin^2\eta_1}\left(p_2^2 + p_3^2 - 2(\cos\eta_1)p_2p_3\right)\right\}. \tag{A3}$$

In the canonical quantization procedure we replace p_i and η_i by operators which act on a Hilbert space of wave functions $\psi(\boldsymbol{\eta})$ defined on the space of Euler angles $\boldsymbol{\eta}$. We require that

$$[\eta_i, p_j] = i\hbar\delta_{ij} \ . \tag{A4}$$

Using a differential representation of the operators $p_i \equiv \frac{\hbar}{i}\frac{\partial}{\partial \eta_i}$, we arrive at the Schrödinger equation

$$\mathcal{H}\psi(\boldsymbol{\eta}) = E\psi(\boldsymbol{\eta}), \tag{A5a}$$

where

$$\mathcal{H} = -\frac{\hbar^2}{2I}\nabla^2_{\mathrm{SO(3)}} \tag{A5b}$$

and the Laplacian operator on SO(3) is given by

$$\nabla^2_{\mathrm{SO(3)}} \equiv \frac{\partial^2}{\partial\eta_1^2} + \cot\eta_1 \frac{\partial}{\partial\eta_1} + \frac{1}{\sin^2\eta_1}\left[\frac{\partial^2}{\partial\eta_2^2} + \frac{\partial^2}{\partial\eta_2^2} - 2\cos\eta_1 \frac{\partial^2}{\partial\eta_2\partial\eta_3}\right]. \tag{A5c}$$

It is straightforward to verify that the third Euler angle η_3 is a cyclic variable which appears neither in the expression for $\mathcal{H}$ nor in the angular momentum operator $\mathbf{L}$. Since p_3 commutes with both $\mathcal{H}$ and $\mathbf{L}$, we may write

$$\psi(\boldsymbol{\eta}) = e^{-i\mu\eta_3}\phi(\eta_1, \eta_2), \tag{A6}$$

where the quantum number μ associated with the conjugate momentum p_3 can be either a half-integer or an integer. These two possibilities correspond to half-integer and integer intrinsic angular momentum states of the spinning top. Half-integer values are allowed because the internal Euler angle space $\boldsymbol{\eta}$ is a topologically, doubly connected manifold. The classical order parameter space for quantum spin $\frac{1}{2}$ is the group manifold of SO(3) rather than the sphere S_2.

A direct comparison of quantum mechanics on SO(3) and quantum mechanics on S_2 is instructive. S_2 may be parametrized by the two angles (η_1, η_2). The gradient operator and Laplacian operators in S_2 are given by

$$\vec{\boldsymbol{\nabla}}_{s_2} = \hat{\eta}_1 \frac{\partial}{\partial\eta_1} + \frac{\hat{\eta}_2}{\sin\eta_1}\frac{\partial}{\partial\eta_2} \tag{A7}$$

and

$$\nabla^2_{s_2} = \frac{\partial^2}{\partial\eta_1^2} + \cot\eta_1\frac{\partial}{\partial\eta_1} + \frac{1}{\sin^2\eta_1}\frac{\partial^2}{\partial\eta_2^2} \ . \tag{A8}$$

It is straightforward to verify that the effects of the Euler angle η_3 are mathematically equivalent to the presence of a gauge field $\mathbf{A} = (0, -\mu\cot\eta_1)$ which acts on the sphere S_2. That is to say, the Schrödinger equation (A5a) may be rewritten as

$$\frac{1}{2I}\left[-(\boldsymbol{\nabla}_{s_2} - i\mathbf{A})^2 + \mu^2\right]\phi(\eta_1, \eta_2) = E\phi \ . \tag{A9}$$

Here, we have made use of (A6). This gauge field is precisely that of a magnetic monopole[44] which sits on the center of the sphere S_2:

$$\boldsymbol{\nabla} \times \mathbf{A} = \mu\hat{r},$$

where $\hat{r}$ is a unit vector in the radial direction.

In (A5) we may look for an internal spin-$\frac{1}{2}$ wave function of the form

$$\psi(\boldsymbol{\eta}) = f(\eta_1)e^{-i(\eta_2+\eta_3)/2} \ . \tag{A10}$$

It is easy to verify that $f(\eta_1) = \cos\eta_1/2$ is a solution for which $E = \frac{3}{4}(\frac{\hbar^2}{2I})$. This wave function is precisely the spin transformation amplitude[14] that an electron in spin $-\hbar/2$ state measured in a laboratory coordinate frame T will be in a $-\hbar/2$ state when the measurement is repeated in a new laboratory coordinate frame S which is related to T by a set of Euler angle rotations $\boldsymbol{\eta}$.

APPENDIX B: EFFECTIVE ONE-ELECTRON HAMILTONIAN FOR A MAGNETIC TEXTURE

In this appendix we present a microscopic derivation of the one-electron continuum Hamiltonian when the local magnetic-moment background has spatial variations. These spatial variations are described by a plaquette orientation vector $\hat{n}(\mathbf{r})$ which varies with $\mathbf{r}$. In this case the SU(2) matrix describing electron hopping between nearest-neighbor sites is given by $T(\mathbf{r}) = -te^{i\frac{\pi}{4}\hat{n}(\mathbf{r})\cdot\sigma}$. From Fig. 4, a typical hopping term is given by

$$\text{Hopping} = \sum_{\mathbf{r}} \left\{ \chi^{\dagger(2)}_{\mathbf{r}+a\hat{\mathbf{x}}} T \chi^{(1)}_{\mathbf{r}} + \chi^{\dagger(2)}_{\mathbf{r}-a\hat{\mathbf{x}}} T \chi^{(1)}_{\mathbf{r}} + \text{H.c.} \right\}. \tag{B1}$$

Here summation is over all plaquettes. Furthermore, $\hat{n}(\mathbf{r})$ is generalized to a continuous vector field which coincides with the required lattice values when $\mathbf{r}$ is at the center of a plaquette. The question now arises, which value of $\hat{n}(\mathbf{r})$ to use in the hopping term. We adopt the convention that for hopping from site $\mathbf{r}$ to site $\mathbf{r}+\mathbf{d}$ we will use $\hat{n}(\mathbf{r}+\mathbf{d}/2)$. Since the variation of $\hat{n}(\mathbf{r})$ within a given plaquette is assumed to be small, the deviations from perfect antiferromagnetic correlation that this choice induces within a given plaquette are likewise very small. As in the uniform state, we make the slowly varying envelope approximation for the field operators in the vicinity of the band edge $\mathbf{k}_0 = \frac{\pi}{2a}(1,1)$ and we write $\chi^{(j)}_{\mathbf{r}} \simeq e^{i\mathbf{k}_0\cdot\mathbf{r}}\tilde{\chi}^{(j)}_{\mathbf{r}}$, where $\tilde{\chi}^{j}_{\mathbf{r}}$ is a slowly varying function with a spectral width $\Delta k \ll k_0$. Making the Taylor expansions

$$\tilde{\chi}^{(j)}_{\mathbf{r}+\mathbf{d}} \simeq \tilde{\chi}^{(j)}_{\mathbf{r}} + (\mathbf{d}\cdot\boldsymbol{\nabla})\tilde{\chi}^{(j)}_{\mathbf{r}} \tag{B2}$$

and

$$T(\mathbf{r}+\mathbf{d}/2) \simeq T(\mathbf{r}) + \frac{1}{2}(\mathbf{d}\cdot\boldsymbol{\nabla})T(\mathbf{r}) \ , \tag{B3}$$

the hopping term has the continuum form

$$\text{Hopping} \simeq -2ia\int d^2\mathbf{r}\Big[(\partial_x\tilde{\chi}^{\dagger(2)})T\tilde{\chi}^{(1)} + \frac{1}{2}\tilde{\chi}^{\dagger(2)}(\partial_x T)\tilde{\chi}^{(1)}\Big] + \text{H.c.} \tag{B4}$$

Integration by parts of the first term yields

$$\text{Hopping} \simeq 2ia\int d^2\mathbf{r}\tilde{\chi}^{\dagger(2)}(T\overleftrightarrow{\partial}_x)\tilde{\chi}^{(1)}, \tag{B5}$$

where the operator $T\overleftrightarrow{\partial}_x$ is defined by

$$(T\overleftrightarrow{\partial}_x)f \equiv \frac{1}{2}[\partial_x(Tf) + T(\partial_x f)] \ . \tag{B6}$$

Comparison of this result with that of the uniform antiferromagnet (T independent of $\mathbf{r}$) reveals that the net effect of a magnetic texture is that the operator $T\partial_x$ must be replaced by the symmetrized, two-way derivative $(T\overleftrightarrow{\partial}_x)$. Applying this argument to each of the hopping terms leads to the generalization

$$\tilde{\alpha}_\mu p_\mu \to \frac{1}{2}[\tilde{\alpha}_\mu(\mathbf{r})p_\mu + p_\mu\tilde{\alpha}_\mu(\mathbf{r})]$$

in the effective one-electron Hamiltonian.

APPENDIX C: MAGNETIC TEXTURES IN TWO DIMENSIONS

In this appendix we begin with the hypothesis that the magnetic twist energy of a texture $\hat{n}(\mathbf{r})$ in the plaquette field is proportional to

$$\mathcal{H}_{\text{mag}} = \frac{1}{2}\int d^2\mathbf{r}(\partial_\mu\hat{n})\cdot(\partial_\mu\hat{n}) \ . \tag{C1}$$

We demonstrate explicitly that the condition for separation of variables in polar coordinates (r,ϕ), of the effective one-electron Hamiltonian, (4.17), is identical to the condition for a local minimum of $\mathcal{H}_{\text{mag}}$.

The topological charge of Q of a texture $\hat{n}(\mathbf{r})$ is defined by the number of times that the vector field $\hat{n}(\mathbf{r})$ covers the sphere S_2 as the coordinate $\mathbf{r}$ covers the two-dimensional Euclidean space:[38]

$$Q = \frac{1}{8\pi}\int d^2\mathbf{r}\hat{n}\cdot[\partial_\mu\hat{n}\times\partial_\nu\hat{n}]\epsilon_{\mu\nu}, \tag{C2}$$

where $\epsilon_{\mu\nu}$ is the standard antisymmetric tensor. We define the auxiliary fields[39]

$$\mathbf{V}^\mu_\pm \equiv \partial_\mu\hat{n} \pm \epsilon_{\mu\nu}(\hat{n}\times\partial_\nu\hat{n}) \tag{C3}$$

and observe that

$$\int d^2\mathbf{r}\mathbf{V}^\mu_\pm(\mathbf{r})\cdot\mathbf{V}^\mu_\pm(\mathbf{r}) \geq 0 \ . \tag{C4}$$

Using the fact that $\hat{n}\cdot\hat{n} = 1$ and $\hat{n}\cdot(\partial_\nu\hat{n}) = 0$, Eq. (C4) may be rewritten as

$$\mathcal{H}_{\text{mag}} \geq 4\pi|Q| \ . \tag{C5}$$

It follows that a local minimum in $\mathcal{H}_{\text{mag}}$, for a fixed value of Q is obtained when the equality in (C4) and (C5) is satisfied. This is the condition that

$$\mathbf{V}^\mu_\pm(\mathbf{r}) = 0, \quad \mu = x,y. \tag{C6}$$

In polar coordinates $\mathbf{r} = (r,\phi)$, the minimization condition (C6) may be reexpressed as

$$\partial_r\hat{n} = \mp\frac{1}{r}(\hat{n}\times\partial_\phi\hat{n}) \tag{C7a}$$

and

$$\frac{1}{r}\partial_\phi\hat{n} = \pm(\hat{n}\times\partial_r\hat{n}) \ . \tag{C7b}$$

We now parametrize the magnetic texture by the winding number μ and a general function $\theta(\mathbf{r})$:

$$\hat{n}(\mathbf{r}) = [\sin\theta\cos(\mu\phi), \sin\theta\sin(\mu\phi), \cos\theta] \ . \tag{C8}$$

Here, it is apparent that $Q = \mu$ and it follows from both Eqs. (C7a) and (C7b) that

$$\partial_r \theta(r) = \pm \frac{\mu}{r} \sin\theta \ . \tag{C9}$$

This is precisely the criterion (4.21) for separation of variables in $\mathcal{H}_{\rm eff}$.

A solution of (C9) is facilitated by the substitution $u(r) \equiv \tan\theta(r)/2$. Direct integration of the differential equation then yields $u(r) = (r/\rho_c)^{\mu s_1}$, $s_1 = \pm 1$. Here ρ_c is a constant of integration which we identify with the soliton core radius. For $\mu = 1$ and $s_1 = +1$, the solution can be reexpressed in terms of $\theta(r)$:

$$\cos\theta(r) = \frac{\rho_c^2 - r^2}{\rho_c^2 + r^2} \quad (\mu = 1) \ . \tag{C10}$$

This is depicted in Fig. 6.

APPENDIX D: SOLUTION OF THE RADIAL SCHRÖDINGER EQUATION

The effective one-electron Hamiltonian for the mean-field spin-flux state, containing a topological magnetic soliton texture, leads to a set of eight coupled, complex, differential equations. This multicomponent Schrödinger equation may be rewritten as a set of purely real differential equations for a radial function $\Psi_{\rm rad}(r)$ by some further unitary transformations. In order to derive these equations, the following identities are useful:

$$\begin{aligned} \tau_y &= e^{-i\tau_z\pi/4}\tau_x e^{i\tau_z\pi/4}, \\ \tau_x &= -e^{-i\tau_z\pi/4}\tau_y e^{i\tau_z\pi/4} \ . \end{aligned} \tag{D1}$$

The Schrödinger equation for the transformed wave function $\psi_5(\mathbf{r}) \equiv e^{i\tau_z\pi/4}\psi_4(\mathbf{r})$ is given by

$$\mathcal{H}\psi_5 = E\psi_5, \tag{D2}$$

where

$$\mathcal{H} = 2ita\left[-\tau_y\partial_r - \gamma_x\frac{\sigma_z\tau_x}{r}(\partial_\phi + is_1\sigma_z/2)\right] + m\beta$$

$$+\frac{ta\mu}{r}[s_1\sin\theta\tau_y\sigma_y - \cos\theta\gamma_x\tau_x] \ . \tag{D3}$$

Since γ_x and $i\partial_\phi$ commute with $\mathcal{H}$, we replace these operators by their eigenvalues $s_2 = \pm 1$ and $\ell = 0, \pm\frac{1}{2}, \pm 1, \ldots$, respectively, to arrive at a matrix equation for $\psi_{\rm rad}(r) \equiv e^{-i\ell\phi}\psi_5(\mathbf{r})$. Multiplying this equation by $i\tau_x$ gives a dimensionless equation in the scaled radius $x \equiv r/a$ and dimensionless energies $\varepsilon \equiv E/2t$, $m \equiv (Us)/2t$:

$$\begin{aligned} \partial_x\psi_{\rm rad}(x) = \Big[&m\sigma_z\tau_x + i\varepsilon\tau_y - \ell s_2\frac{\sigma_z\tau_z}{x} \\ &+\left(\frac{\mu\cos\theta - s_1}{2x}\right)s_2\tau_z \\ &-i\mu s_1\left(\frac{\sin\theta}{2x}\right)\sigma_y\Big]\psi_{\rm rad}(x) \ . \end{aligned} \tag{D4}$$

Solutions of this equation are determined by imposing the condition that the original (physical) wave function

$$\begin{aligned} \psi_0(\mathbf{r}) = &\frac{1}{\sqrt{r}}e^{i\ell\phi}U^\dagger(\mathbf{r})e^{-i\alpha_z\phi/2} \\ &\times e^{is_1\sigma_z\phi/2}e^{-is_1\gamma_x\sigma_x\pi/8} \\ &\times e^{-i\sigma_z\tau_z\pi/4}e^{-i\tau_z\pi/4}\psi_{\rm rad}(r) \end{aligned} \tag{D5}$$

is nonsingular as $r \to 0$ and as $r \to \infty$.

We begin by considering a Skyrmion texture with topological charge $|\mu| = 1$. From Appendix C, we observe that $\lim_{r\to 0}\cos\theta(r) = \frac{\mu s_1}{|\mu s_1|}$. It follows that the final two terms in Eq. (D4) are regular at the origin: $(\mu\cos\theta - s_1) = s_1[(\mu s_1)\cos\theta - 1] \to 0$ and $\mu s_1 \sin\theta \to 0$ as $r \to 0$. If we allow $\ell = 0$, then all terms in (D4) will be nonsingular and $\psi_{\rm rad}(r)$ will likewise be regular at $r = 0$. From (D5), we see that this would result in a square root singularity in the physical wave function $\psi_0(\mathbf{r})$.

It follows that there are no admissible solutions for the quantum number $\ell = 0$. Next we consider $\ell = \frac{1}{2}$. In this case, the third term in (D4) is dominant as $x \to 0$. For small x, we have

$$\ell = \frac{1}{2}, \quad \partial_x\psi_{\rm rad} \simeq -s_2\left(\frac{\sigma_z\tau_z}{2x}\right)\psi_{\rm rad} \ . \tag{D6}$$

The eigenvalues of $\sigma_z\tau_z$ are doubly degenerate and equal to ± 1. Suppose that $s_2 = +1$. Then for small x the solution of (D6) has the asymptotic form $\psi_{\rm rad} \sim x^{\pm 1/2}$. Clearly, we must choose the positive eigenvalues of $\sigma_z\tau_z$ in order that $\psi_0(\mathbf{r})$ in (D5) is regular at the origin. Let v_1 and v_2 be the eigenvectors of $\sigma_z\tau_z$ corresponding to the required positive eigenvalue. Then, $\psi_{\rm rad}(0) = a_1v_1 + a_2v_2$ for arbitrary coefficients a_1 and a_2. For large x, (D4) has the asymptotic form

$$\partial_x\psi_{\rm rad} \simeq (m\sigma_z\tau_x + i\epsilon\tau_y)\psi_{\rm rad}, \quad x \to \infty \ . \tag{D7}$$

The eigenvalues of the matrix $(m\sigma_z\tau_x + i\varepsilon\tau_y) \equiv M$ are given by $\lambda_\pm \equiv \pm(m^2 - \varepsilon^2)^{1/2}$. If $\psi_{\rm rad}$ is a normalizable wave function, only the negative eigenvalue is admissible. Let ω_1 and ω_2 be eigenvectors of M corresponding to λ_+ and ω_3 and ω_4 be eigenvectors of M corresponding to λ_-. $\omega_1, \ldots, \omega_4$ form a complete orthormal basis of the vector space spanned by the $\boldsymbol{\sigma}$ and $\boldsymbol{\tau}$ matrices. It follows that $\psi_{\rm rad}(x)$ may be expanded as a linear combination of these eigenvectors at some arbitrary radius x. For instance, if we numerically integrate the first-order differential equation (D4) using the initial condition $\psi_{\rm rad}(0) = v_1$, the result at any point $x > 0$ may be represented as $\psi_{\rm rad}(x) = \sum_{j=1}^4 c_{1j}\omega_j$ for some numerical coefficients c_{1j}. Likewise if we choose $\psi_{\rm rad}(0) = v_2$, there exists another set of coefficients c_{2j}, such that $\psi_{\rm rad}(x) = \sum_{j=1}^4 c_{2j}\omega_j$. We consider the asymptotic (large x) behavior of the coefficients $c_{ij}(\varepsilon)$ which depend implicitly on the energy ε. For $\psi_{\rm rad}$ to be normalizable, we may now use our freedom in the coefficients a_1 and a_2 which define $\psi_{\rm rad}(0)$. That is to say, a_1 and a_2 must be chosen such that

$$\psi_{\rm rad}(x) \sim a_1\sum_{j=1}^4 c_{1j}(\varepsilon)\omega_j + a_2\sum_{j=1}^4 c_{2j}(E)\omega_j$$

(for large x)

does not contain the eigenvectors ω_1 and ω_2 corresponding to exponentially growing solutions. Using the fact that ω_1 and ω_2 are linearly independent vectors, the above considerations yield the condition that

$$C(\varepsilon)\begin{pmatrix} a_1 \\ a_2 \end{pmatrix} = 0,$$

where the 2×2 matrix

$$C(\varepsilon) \equiv \begin{bmatrix} c_{11}(\varepsilon) & c_{21}(\varepsilon) \\ c_{12}(\varepsilon) & c_{22}(\varepsilon) \end{bmatrix}.$$

This yields the required eigenvalue condition that $\det C(\varepsilon) = 0$. A similar algorithm may be used to determine the eigenvalue spectrum for other values of ℓ and for magnetic solitons with higher topological charge μ. The results are plotted in Figs. 7–9.

[1] J.G. Bednorz and K.A. Muller, Z. Phys. B **64**, 189 (1986).
[2] P.W. Anderson, Science **235**, 1196 (1987).
[3] See, for instance, D.M. Ginsberg, *Physical Properties of High Temperature Superconductors* (World Scientific Press, Singapore, 1992), Vols. I–III.
[4] P.W. Anderson and J.R. Schrieffer, Physics Today **44**, 55 (1991).
[5] H.A. Bethe, Z. Phys. **71**, 205 (1931); L. Hulthen, Ark. Mat. Astron. Fys. **26A**, 11 (1938).
[6] J. des Cloizeaux and J.J. Pearson, Phys. Rev. **128**, 2131 (1962); Y. Endoh *et al.*, Phys. Rev. Lett. **32**, 170 (1974).
[7] See, for instance, E. Lieb, T. Schultz, and D. Mattis, Ann. Phys. (N.Y.) **16**, 407 (1961).
[8] J.M. Luttinger, J. Math. Phys. **15**, 609 (1963); F.D.M. Haldane, J. Phys. C **14**, 2585 (1981).
[9] J.R. Schrieffer, X.G. Wen, and S.C. Zhang, Phys. Rev. B **39**, 11 663 (1989).
[10] B.I. Shraiman and E.D. Siggia, Phys. Rev. B **40**, 9162 (1990).
[11] N. Rosen, Phys. Rev. **82**, 621 (1951).
[12] L. Schulman, Phys. Rev. **176**, 1558 (1968).
[13] See, for instance, H. Goldstein, *Classical Mechanics* (Addison-Wesley, New York, 1980).
[14] For an alternative derivation from purely geometric arguments, R. P. Feynman, R. B. Leighton, and M. Sands, *Feynman Lectures in Physics Vol. 3* (Addison-Wesley, Reading, MA, 1966), Chap. 6.
[15] A.W. Overhauser, Phys. Rev. **128**, 1437 (1962).
[16] S. John and P. Voruganti, Phys. Rev. B **43**, 13 365 (1991).
[17] S. John, P. Voruganti, and W. Goff, Phys. Rev. B **43**, 10 815 (1991).
[18] P. Voruganti, A. Golubentsev, and S. John, Phys. Rev. B **45**, 13 945 (1992).
[19] N.D. Mermin and H. Wagner, Phys. Rev. Lett. **17**, 1133 (1966).
[20] G. Shirane *et al.*, Phys. Rev. B **41**, 6547 (1990).
[21] S.M. Hayden *et al.*, Phys. Rev. Lett. **66**, 821 (1991).
[22] T.R. Thurston *et al.*, Phys. Rev. B **40**, 4585 (1989); G. Shirane *et al.*, Phys. Rev. Lett. **63**, 330 (1989); R.J. Birgeneau *et al.*, Phys. Rev. B **38**, 6614 (1988).
[23] S.W. Cheong *et al.*, Phys. Rev. Lett. **27**, 1791 (1991).
[24] Z.Z. Wang *et al.*, Phys. Rev. B **43**, 3020 (1991); H. Takagi *et al.*, Phys. Rev. Lett. **62**, 1197 (1989); N.P. Ong *et al.*, Phys. Rev. B **35**, 8807 (1987).
[25] C.M. Varma *et al.*, Phys. Rev. Lett. **64**, 497 (1990).
[26] P.W. Anderson, Phys. Rev. Lett. **64**, 1839 (1990).
[27] This was originally suggested in S. John and A. Golubentsev, Phys. Rev. Lett. **71**, 3343 (1993).
[28] N.F. Mott, Proc. Phys. Soc. London, Sect. A **62**, 416 (1949); Rev. Mod. Phys. **40**, 677 (1968).
[29] J. Hubbard, Proc. R. Soc. London, Ser. A **276**, 238 (1963).
[30] I. Affleck and B. Marston, Phys. Rev. B **37**, 3774 (1988); B. Marston and I. Affleck, *ibid.* **39**, 11 538 (1989).
[31] G.B. Kotliar, Phys. Rev. B **37**, 3664 (1988).
[32] G. Baskaran, Z. Zou, and P.W. Anderson, Solid State Commun. **63**, 973 (1987).
[33] F. Wilczek, Phys. Rev. Lett. **49**, 957 (1982); R.B. Laughlin, Science **242**, 525 (1988).
[34] D.C. Morse and T.C. Lubensky, Phys. Rev. B **43**, 10 436 (1991).
[35] D. Finkelstein and J. Rubinstein, J. Math. Phys. **9**, 1762 (1968).
[36] P. Wiegmann, Prog. Theor. Phys. Suppl. **107**, 243 (1992).
[37] D.V. Khveshchenko and P.B. Wiegmann, Mod. Phys. Lett. B **3**, 1383 (1989); **4**, 17 (1990).
[38] A.M. Polyakov, *Gauge Fields and Strings* (Harwood Academic Publishers, Chur, Switzerland, 1987).
[39] R. Rajaraman, *Solitons and Instantons* (North-Holland Physics Publishing, Amsterdam, 1987).
[40] S. Uchida *et al.*, Phys. Rev. B **43**, 7942 (1991).
[41] D.B. Tanner and T. Timusk, in *Physical Properties of High-Temperature Superconductors III,* edited by D. Ginsberg (World Scientific, Singapore, 1992); G.A. Thomas, *Proceedings of the 39th Scottish Universities Summer School in Physics,* St. Andrews (Adam Hilger, New York, 1991).
[42] J.D. Perkins *et al.*, Phys. Rev. Lett. **71**, 1621 (1993).
[43] See, for instance, R.B. Laughlin, in *The Quantum Hall Effect,* edited by R. Prange and S. Girvin (Springer-Verlag, Berlin, 1987).
[44] J.M. Leinaas, Phys. Scr. **17**, 483 (1978).